1973-06

An application of the piecewise-sinusoidal reaction matching technique to linear dipole antennas

Bryant, Michael Lynn

Monterey, California. Naval Postgraduate School

AN APPLICATION OF THE PIECEWISE-SINUSOIDAL REACTION MATCHING TECHNIQUE TO LINEAR DIPOLE ANTENNAS

Michael Lynn Bryant

NAVAL POSTGRADUATE SCHOOL
Monterey, California

THESIS

AN APPLICATION OF THE PIECEWISE-SINUSOIDAL
REACTION MATCHING TECHNIQUE
TO LINEAR DIPOLE ANTENNAS

by

Michael Lynn Bryant

Thesis Advisor: R.W. Adler

June 1973

An Application of the Piecewise-Sinusoidal Reaction Matching Technique to Linear Dipole Antennas

by

Michael Lynn Bryant
Ensign, United States Navy
B.S.E.E., United States Naval Academy, 1972

Submitted in partial fulfillment of the
requirements for the degree of

MASTER OF SCIENCE IN ELECTRICAL ENGINEERING

from the

NAVAL POSTGRADUATE SCHOOL

June 1973

ABSTRACT

This paper is an application of the Piecewise-Sinusoidal Reaction Matching Technique (PSRMT) to linear, parallel thin-wire dipoles. The "method of moments" if briefly outlined and the fundamental electromagnetic principles of reciprocity, surface equivalence and reaction are discussed. Through a logical combination of these concepts, PSRMT is developed and applied to thin-wire dipoles radiating in free space due to a delta function voltage generator at their center. The driving point impedance and the current distribution are calculated and compared to results obtained from other independent theoretical techniques.

The major contribution of this investigation is not that of presenting a new technique for calculating the input impedance and current distributions on dipole antennas. The study is primarily concerned with comparing other well-known techniques with that of PSRMT. Emphasis is placed on the ease and convenience of expressing the mutual impedance integrals of coplanar dipoles in closed form.

TABLE OF CONTENTS

LIST OF TABLES

LIST OF ILLUSTRATIONS

ACKNOWLEDGEMENTS

The author is indebted to a multitude of persons for their assistance and patience during the preparation of this thesis. Foremost, I wish to thank Dr. Richard W. Adler, under whose direct supervision I worked. Without his patient guidance, sense of humor and tireless enthusiasm this work would not have been accomplished. Secondly, I wish to convey my sincere thanks to Dr. Jack H. Richmond of the University of Ohio for his encouragement and assistance.

I wish to express my thanks to Eugene G. Neely for his witty and frequent aid. Thanks is also due my wife, Monica, for her confidence and assurance throughout this project.

All computer calculations were conducted at the W. R. Church Computer Center. The cooperation of the Computer Center staff is appreciated.

I. INTRODUCTION

A. DESCRIPTION OF ANTENNA PROBLEM UNDER INVESTIGATION

This paper is an investigation of the efficiency of the Piecewise-Sinusoidal Reaction Matching Technique (PSRMT). In the solution of problems using the "method of moments" [3], computation time on the computer depends primarily upon the amount of computational effort required to generate the elements in the generalized impedance matrix. Usually this relates to the amount of numerical integration required to calculate the Z_{mn}'s. However, by employing piecewise-sinusoidal basis functions to obtain the impedance matrix, closed form expressions can be obtained for the integrations. Also, the size of the impedance matrix required to adequately solve the antenna problem is relatively small when compared to the use of other basis and weighting functions. For these reasons PSRMT will be applied and the results compared to other techniques.

The antenna configuration under investigation will be restricted to a linear, thin-wire dipole. The antenna is assumed to be radiating in free space and is driven at the center by a delta function voltage generator. In this particular application of PSRMT, all segments of the filamentary dipoles are parallel and of equal length. This is not a necessary condition, but one of convenience. The

driving point impedance and the current distributions will be calculated by an application of PSRMT.

B. BRIEF HISTORY OF RELATED WORK

In the past much work has been done in the area of determining the mutual impedance between two elements with an assumed sinusoidal current distribution. Carter [5] has presented the mutual impedance between two wires in echelon where each antenna is an odd number of half-wavelengths long. The mutual impedance expression between two identical nonstaggered parallel center-fed antennas of Brown [1] is of historical renown. The work of Brown was carried one step further by Cox [6] who developed the mutual impedance between parallel antennas of unequal lengths.

In 1957, H. E. King published a paper [10] that developed an expression for the mutual impedance between two staggered parallel, center-fed, infinitely thin antennas of unequal lengths. Lewin [12] analyzed the mutual impedance of two coplanar half-wave dipoles, in arbitrary positions. Finally Lewin's work was generalized by Richmond and Geary [10] for any length antenna.

All of the above studies were restricted to assumed sinusoidal dipole current distributions. Without assuming a current distribution upon an antenna the current distribution may be found by breaking the antenna up into several segments, calculating the mutual impedance between each pair of elements in turn and generating an impedance matrix

that characterizes the current distribution. This calculation of the mutual impedance is done in general by the expression published by Richmond and Geary. The technique crudely described is that of reaction matching.

C. SCOPE AND LIMITATIONS OF THE STUDY

This paper develops the multisegment reaction technique from fundamental electromagnetic theory. Although the technique is applied only to linear thin-wire dipoles of perfect conductivity, the procedure may be extended to more general and intricate geometries. To cite one of the many examples, PSRMT has been successfully employed by Travieso-Diaz [20] to the analysis of antennas and scatterers with arbitrary surface shape.

II. OUTLINE OF THE METHOD OF MOMENTS

The following discussion portrays the major steps employed in the method of moments. The object is to reduce the functional equations of field theory to matrix equations which can be readily solved. The name "method of moments" has been given to the mathematical procedure for obtaining the matrix equations [8].

A. FORMULATION OF THE OPERATOR EQUATION

Consider only equations of the inhomogenous type $L(\overline{f}) = \overline{g}$, where L is a given operator, $\overline{g}$ is the excitation or source (known function), and $\overline{f}$ is the field or response (unknown to be determined).

One must determine from physical considerations that the problem in question is deterministic, that is, if the solution for $\overline{f}$ when L and $\overline{g}$ are given is unique. The method of moments gives a general procedure for treating field problems, but the details of solution vary widely with the particular problem. The analysis to follow is that which is germane to the antenna problem under investigation.

B. POSTULATION OF THE BASIS FUNCTION

Consider the deterministic equation

$$L(\overline{f}) = \overline{g} \ , \tag{1}$$

where L is a linear operator, $\bar{g}$ is known, and $\bar{f}$ is to be determined. Let $\bar{f}$ be expanded in a series of functions or a linear combination of a set of N vectors $\{\bar{f}_n\}$

$$\bar{f} = \sum_n c_n \bar{f}_n \quad , \tag{2}$$

where the c_n's are constants that are not known but are to be determined in the solution process. The $\bar{f}_n$'s are chosen to be linearly independent and are called expansion functions or basis functions. For exact solutions, Equation (2) is usually an infinite summation and $\bar{f}_n$'s form a complete set of basis functions. For approximate solutions, Equation (2) is usually a finite summation. Substituting Equation (2) into Equation (1), and using the linearity property of L,

$$\sum_n c_n L(\bar{f}_n) = \bar{g} \quad . \tag{3}$$

C. POSTULATION OF THE WEIGHTING FUNCTION

It is assumed at this point that a suitable inner product $\langle f,g \rangle$ has been determined for the problem. The inner product is a scalar defined to satisfy

$$\langle f,g \rangle = \langle g,f \rangle$$

$$\langle \alpha f + \beta g,h \rangle = \alpha \langle f,h \rangle + \beta \langle g,h \rangle$$

$$\langle f^*,f \rangle > 0, \quad \text{if } f \neq 0$$
$$= 0, \quad \text{if } f = 0 \ ,$$

where α and β are scalars, and * denotes complex conjugate [8]. The appropriate inner product for this particular antenna problem will be developed in the section of this paper entitled "Reaction Concept". Now define a set of M linearly independent weighting or testing vectors $\{\bar{w}_m\}$, and take the inner product of Equation (3) with each $\bar{w}_m$. The result is

$$\sum_n c_n \langle \bar{w}_m, L\bar{f}_n \rangle = \langle \bar{w}_m, \bar{g} \rangle \qquad (4)$$

m = 1, 2, 3, ... M, where the N c_n's are unknown and all other terms are known [3].

D. SOLUTION OF THE LINEAR ALGEBRAIC SYSTEM

Equation (4) can be written in matrix form as

$$\left[\ell_{mn}\right] \left[c_n\right] = \left[\bar{g}_n\right] , \qquad (5)$$

where

$$\left[\ell_{mn}\right] = \begin{bmatrix} \langle \bar{w}_1, L\bar{f}_1 \rangle & \langle \bar{w}_1, L\bar{f}_2 \rangle & \cdots \\ \langle \bar{w}_2, L\bar{f}_1 \rangle & \langle \bar{w}_2, L\bar{f}_2 \rangle & \cdots \\ \cdots & \cdots & \cdots \end{bmatrix} ,$$

$$\left[c_n\right] = \begin{bmatrix} c_1 \\ c_2 \\ c_3 \\ \cdot \\ \cdot \end{bmatrix} \quad \text{and} \quad \left[\overline{g}_n\right] = \begin{bmatrix} \overline{w}_1, \overline{g} \\ \overline{w}_2, \overline{g} \\ \overline{w}_3, \overline{g} \\ \cdot \\ \cdot \end{bmatrix} .$$

A consistent equation results by requiring M and N to be equal. That is, the basis set $\overline{f}_n$ and the testing set $\overline{w}_m$ each has N elements. The coefficient matrix is determined by inversion:

$$\left[c_n\right] = \left[\overline{\ell}_{mn}\right]^{-1} \left[\overline{g}_m\right] \tag{6}$$

provided that the matrix $\left[\overline{\ell}_{mn}\right]$ is nonsingular. The solution for $\overline{f}$ is given by Equation (2):

$$\overline{f} = \left[\overline{f}_n\right] \left[c_n\right] . \tag{7}$$

This solution may be exact or approximate, depending upon the choice of $\overline{f}_n$ and $\overline{w}_m$ and the extent of the summation. The particular choice $\overline{w}_m = \overline{f}_n$ is known as Galerkin's method.

E. COMMENTARY ON THE METHOD OF MOMENTS

One of the most critical tasks in any particular problem is the choice of the basis and testing functions, $\overline{f}_n$ and $\overline{w}_m$. The $\overline{f}_n$'s should be linearly independent and chosen so

that some superposition (see Equation (2)) can approximate $\overline{f}$ reasonably well. The $\overline{w}_m$'s should also be linearly independent and chosen so that the products $\langle \overline{w}_m, \overline{g} \rangle$ depend on relatively independent properties of $\overline{g}$. Obviously additional considerations affecting the choice of $\overline{f}_n$ and $\overline{w}_m$ are a.) the accuracy of solution desired, b.) the ease of evaluation of the matrix elements, c.) the size of the matrix that can be inverted, and d.) the realization of a well-conditioned matrix $[\ell_{mn}]$ [8].

F. PIECEWISE-SINUSOIDAL BASIS SETS

The physical problem may be represented by many different operator equations, and a suitable one must be chosen. There are also an infinite number of sets of expansion functions $\overline{f}_n$ and testing functions $\overline{w}_m$ that may be chosen.

Intuitively, the more nearly the expansion set resembles the actual form of the current distribution, the fewer the terms required to accurately represent the current. In addition, certain types of basis functions may lessen many time-consuming, numerical operations incorporated in approximations. The piecewise-sinusoidal basis set exhibits these qualities. The objective is to represent the current distribution, over individual subsections of a domain with expansion functions that possess greater curve-fitting potential than do flat pulses and yet lead to well-conditioned matrices in approximate solution procedures. The application

of piecewise-sinusoids in Galerkin's method and the method of moments to electromagnetic field problems is known as the reaction concept [3,17].

III. THEORETICAL MOTIVATION

The following discussion will develop the basic concept utilized in the formulation of the reaction matching technique of J. H. Richmond. The reaction concept of Rumsey [17], the reciprocity principle [9] and the surface equivalence theorem [18] were presented by Richards [13] and Travieso-Diaz [20]. The concepts of reciprocity, reaction and surface equivalence form the theoretical motivation for PSRMT; therefore they are included again here. With a logical combination of these elements, one can develop a general formulation of electromagnetic boundary-value problems, in particular, reaction matching.

A. RECIPROCITY THEOREMS

Consider a pair of time-harmonic sources of the same frequency ω radiating in a linear, isotropic, but not necessarily homogenous medium with permittivity ϵ and permeability μ. One of the sources, designated as source 1, has impressed electric and magnetic current densities $(\bar{J}_1, \bar{M}_1)$ which radiate fields $(\bar{E}_1, \bar{H}_1)$ in the presence of a second source, source 2, acting as a receiver. Similarly, the current densities $(\bar{J}_2, \bar{M}_2)$ of source 2 set up fields $(\bar{E}_2, \bar{H}_2)$ in the presence of source 1 acting as a receiver.

The fields of these sources at every point in the medium are related by the point reciprocity theorem of Lorentz [9] as follows:

$$\nabla \cdot (\bar{E}_1 \times \bar{H}_2 - \bar{E}_2 \times \bar{H}_1) = (\bar{J}_1 \cdot \bar{E}_2 - \bar{J}_2 \cdot \bar{E}_1) - (\bar{M}_1 \cdot \bar{H}_2 - \bar{M}_2 \cdot \bar{H}_1) \tag{8}$$

Now let the sources be of finite extent, and assume all inhomogeneities in the medium to have a finite distribution. Define non-overlapping surfaces S_1 and S_2 enclosing the source distributions $(\bar{J}_1, \bar{M}_1)$ and $(\bar{J}_2, \bar{M}_2)$ respectively; all inhomogeneities are contained in the volumes V_1 and V_2 bounded by S_1 and S_2. Therefore, the medium outside S_1 and S_2 is homogeneous. Under these conditions, the reciprocity theorem of Carson [4] establishes a relation between the source distributions $(\bar{J}_1, \bar{M}_1)$ and $(\bar{J}_2, \bar{M}_2)$ and the fields $(\bar{E}_1, \bar{H}_1)$ and $(\bar{E}_2, \bar{H}_2)$ of Equation (8) as

$$\iiint_{V_1} (\bar{J}_1 \cdot \bar{E}_2 - \bar{M}_1 \cdot \bar{H}_2) dv = \iiint_{V_2} (\bar{J}_2 \cdot \bar{E}_1 - \bar{M}_2 \cdot \bar{H}_1) dv . \tag{9}$$

B. SURFACE EQUIVALENCE PRINCIPLE

The surface equivalence principle can be briefly described as follows [13]. First, an original source distribution $(\bar{J}_i, \bar{M}_i)$ set up fields $(\bar{E}, \bar{H})$ everywhere in some defined medium. Next, the original source is turned off, but simultaneously surface current densities $(\bar{J}_s, \bar{M}_s)$ are set up on a surface S which encloses the original

source and any inhomogeneities. If the surface current densities ($\bar{J}_s$, $\bar{M}_s$) are related to the original fields ($\bar{E}$, $\bar{H}$) by

$$\bar{J}_s = \hat{n} \times \bar{H} \tag{10A}$$

$$\bar{M}_s = \bar{E} \times \hat{n} \quad , \tag{10B}$$

where $\hat{n}$ is the unit normal at S directed outward from S, then these surface current distributions will radiate the original fields ($\bar{E}$, $\bar{H}$) in the region exterior to the surface S and will generate a null field inside S.

C. REACTION CONCEPT

In 1954 V. H. Rumsey published a paper [17] in which he introduced a new physical observable, "reaction". Define a complex number denoted by $\langle a, b \rangle$ as follows:

$$\langle a, b \rangle = \iiint_V [\bar{J}(a) \cdot \bar{E}(b) - \bar{M}(a) \cdot \bar{H}(b)] dv, \tag{11}$$

where the volume V contains the source a.

The reciprocity theorem states that

$$\langle a, b \rangle = \langle b, a \rangle \tag{12}$$

provided that all media are isotropic and that a and b can be contained in a finite volume. The scalar $\langle a, b \rangle$ is

a measure of the reaction (or coupling) between the sources a and b. Equation (11) is to be understood as a formula for the measure of reaction. It is obvious that Equation (9) may be restated as Equation (12), where the inner product represents the complex integrals of Equation (9). Equation (12) is, therefore, the reaction form of reciprocity. These theorems will now be used to develop the "Piecewise Sinusoidal Reaction Matching Technique" (PSRMT) of J. H. Richmond.

IV. PIECEWISE-SINUSOIDAL REACTION MATCHING TECHNIQUE (PSRMT)

A. INTRODUCTION TO PSRMT

In this section, the method of moments and the reaction concept will be applied to the solution of the current distribution on linear antennas. This particular class of problem involves only antennas which consist of or can be represented by a collection of thin-wire segments.

An axial filamentary test source will be developed. After specifying a suitable current distribution on both the original and the test antenna, the reaction concept will be applied. Reaction will be employed in order to develop a system of linear equations whose solution will yield the complex coefficients that complete the description of the approximate current distribution specified.

The reaction concept and its applications have been discussed by Rumsey [17] and Harrington [9]. The interpretation of PSRMT to follow is primarily that of Richards [13] and Leonard Tsai [21]. Most of the material presented here has been previously presented by Richmond [14, 15, 16] and Richards; it is presented here for completeness.

B. THIN-WIRE PROBLEM

Consider the thin-wire dipole shown in Figure 1. The dipole arms are wire segments of length L_1 and L_2, not necessarily equal, but shorter than $\lambda/2$. The radius "a"

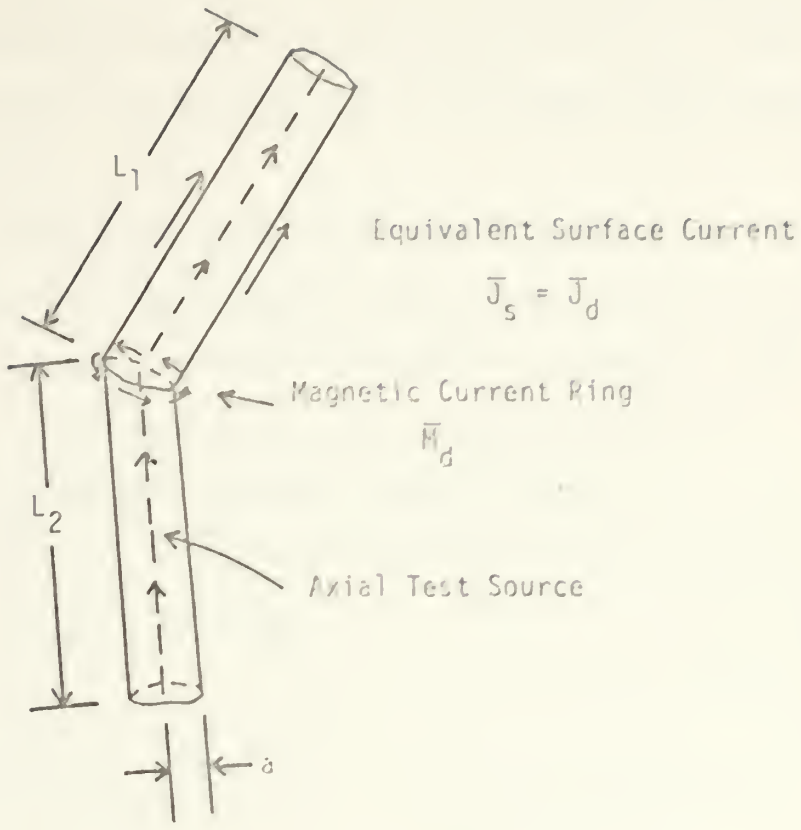

FIGURE 1. A thin-wire dipole with a filamentary test source on its axis.

of the wire is arbitrary, but in the thin-wire case always small in terms of λ; also, $a \ll L_1$ and $a \ll L_2$. The dipole is driven at the junction of its arms with a magnetic ring current $\bar{M}_d$.

Let the dipole depicted in Figure 1 radiate in free space, setting up time-harmonic field intensities ($\bar{E}_d$, $\bar{H}_d$) everywhere. By the surface equivalence principle this antenna may be replaced by a set of surface currents ($\bar{J}_d$, $\bar{M}_d$) enclosing the primary source where

$$\bar{J}_d = \hat{n} \times \bar{H}_d \tag{13A}$$

$$\bar{M}_d = \bar{E}_d \times \hat{n} \tag{13B}$$

at the surface, and $\hat{n}$ is the unit normal vector pointing outward from the surface. Let this surface exist at an infinitesimal distance outwardly away from the actual dipole, so that the dipole itself is replaced by surface currents ($\bar{J}_d$, $\bar{M}_d$). Then it is known that exterior to this surface the two fields ($\bar{E}_d$, $\bar{H}_d$) exist and there is a null field inside the surface. Now the original source can be removed without disturbing the fields, so that there is free space everywhere.

A test source is placed at the axis of the actual dipole in Figure 1, in order to employ the reaction test. Alone, this filamentary test dipole radiates the fields

$(\bar{E}_t, \bar{H}_t)$ in free space. The Carson reciprocity theorem of Equation (9) may be applied between the test dipole and the unknown equivalent surface current on the original dipole to give:

$$\iint_{S_e} [J_d \cdot E_t - M_d \cdot H_t] ds_e = \int_{\ell} [I_t \cdot E_d - M_t \cdot H_d] d\ell \ , \tag{14}$$

where S_e is the surface of the original dipole as shown in Figure 1, ℓ is the coordinate along the filamentary test dipole, and $(\bar{I}_t, \bar{M}_t)$ represents the currents of the test dipole. Due to the null field generated by the original source in the interior of S_e, where the coordinate along the filamentary test dipole is, the right-hand side of Equation (14) is identically zero. Therefore the reaction between the two sources is zero,

$$\langle a, b \rangle \equiv \langle b, a \rangle \equiv 0 \ ,$$

hence the term "zero reaction condition". This zero reaction theorem was developed by Rumsey [17]. Equation (14) written in light of the zero reaction condition is:

$$\iint_{S_e} \bar{M}_d \cdot \bar{H}_t \, ds_e = \iint_{S_e} \bar{J}_d \cdot \bar{E}_t \, ds_e \ . \tag{15}$$

For a typical antenna problem, the excitation consists of a voltage generator driving the dipole at the junction

of its arms. Since the antenna is thin, a "delta gap" voltage generator is assumed. Here the impressed current densities are:

$$\bar{J}_d = 0 \tag{16A}$$

$$\bar{M}_d = \phi\,(\delta - a,\ \ell - \ell_0)V_d \ , \tag{16B}$$

where V_d is the strength of the voltage generator, "a" is the radius, ℓ_0 is the value of the coordinate ℓ at the gap and δ is the Dirac delta function.

In this case $\bar{M}_d$ is a ring of magnetic current at the terminals, and the integral on the left-hand side of Equation (15) reduces to a line integral. Applying Ampere's law to perform the integration around the gap:

$$\iint_{S_e} \bar{M}_d \cdot \bar{H}_t \, ds_e = -a\, V_d \int_0^{2\pi} \bar{H}_t(a, \ell_0, \phi)\, d\phi$$

$$= -V_d\, I_t\,(\ell_0) \ . \tag{17}$$

Combining Equations (15) and (17) yields

$$\iint_{S_e} J_d \cdot E_t \, ds_e = -V_d\, I_t\,(\ell_0) \tag{18}$$

where $I_t\,(\ell_0)$ is the complex terminal current on the test dipole.

For the evaluation of Equation (18) allow the thin-wire approximation ($a \ll \lambda$) to hold, thus the distribution of current density may be assumed to be uniform around the cylinder. This assumption may be expressed mathematically as simply, $\bar{J}_d = \bar{I}_d/2\pi a$ where "a" is the radius and $\bar{I}_d$ varies only along the length of the dipole. Thus Equation (18) becomes

$$V_d = -\frac{1}{\bar{I}_t} \int_{\ell_e} \bar{I}_d (\ell_e) \bar{E}_t \, d\ell_e \quad . \tag{19}$$

Equation (19) is the result of replacing the surface current density $\bar{J}_d$ with an equivalent filamentary current of strength $\bar{I}_d = 2\pi a \bar{J}_d$ which is located on the previous surface where $\bar{J}_d$ resides. The integration $d\ell_e$ is along this line on the dipole surface and $\bar{E}_t$ represents the field of the test dipole on this line. It should be noted that if the test dipole were not axially located, then this simplification would not be judicious.

Equation (19) forms the foundation upon which the two segment reaction matching technique is based. Once V_d is specified and the current distribution $\bar{I}_d$ is assumed, the coefficients for the current $\bar{I}_d$ may be readily determined. For the remainder of this paper the discussion will involve current distributions on both the test dipole and on the original dipole that are "piecewise-sinusoidal" in form. This will lead to considerable simplification because

a.) closed form expressions for the $\bar{E}_t$ term can be found, and b.) closed form expressions for $\int \bar{I}_d \cdot \bar{E}_t \, d\ell_e$ also exist for coplanar dipoles. The basis for these claims will be presented after a generalization is made for N segment reaction matching.

An essential feature of any acceptable test source ($\bar{J}_t$, $\bar{M}_t$) must be that the fields it radiates be known and, if possible, that they be known in closed form. One such source is a filamentary electrical source with time-harmonic current, as shown in Figure 2.

Let the source be located on the z axis with endpoints z_1 and z_2, and the current distribution be of the form:

$$I(z) = A\, e^{jkz} + B\, e^{-jkz} , \tag{20}$$

where A and B are complex constants, $k = 2\pi/\lambda$, and the time dependence $e^{j\omega t}$ is understood and suppressed.

C. ELECTRIC FIELDS OF A PIECEWISE-SINUSOIDAL FILAMENTARY SOURCE

As expression for the z component of the free-space electric field of the filamentary source of Figure 2 is given by Schelkunoff and Friis [19] as

$$E_z = \frac{1}{4\pi j\omega\varepsilon}\left[I_1' \frac{e^{-jkR_1}}{R_1} - I_2' \frac{e^{-jkR_2}}{R_2} - \frac{\partial V}{\partial z} \right]. \tag{21}$$

Here $I_1 = I(z_1)$, $I_1' = I'(z_1)$, $I_2 = I(z_2)$, $I_2' = I'(z_2)$,

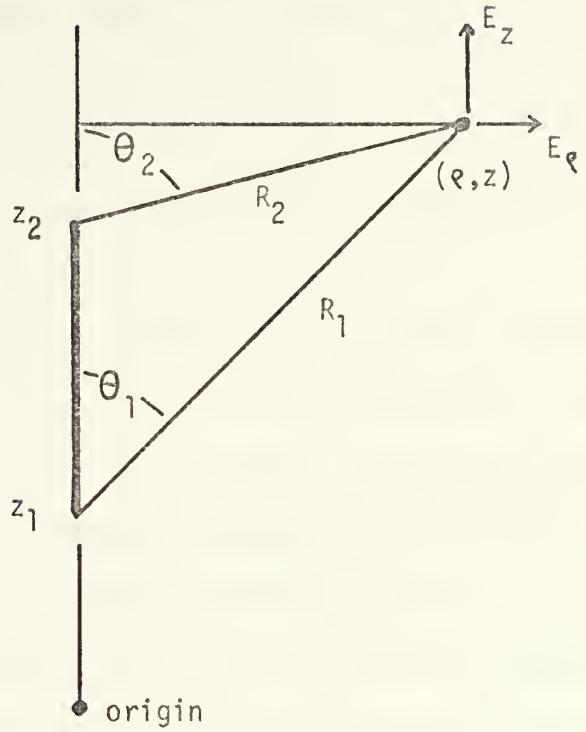

Figure 2. Filamentary electric line source on the z axis sets up a field (E_ρ, E_z) at an observation point (ρ,z).

and V is the electric potential of the end charges; ε is the permittivity of the medium. Throughout this paper the prime denotes taking the derivative with respect to z.

The electric field $\bar{E}_t$ is composed of both a normal component E_ρ and a tangential component E_z as depicted in Figure 2.

Note that in performing the dot product "$\bar{J}_d \cdot \bar{E}_t$" of Equation (18) for linear antennas, only the z component of the electric field makes a contribution. That is the justification for ignoring the E_ρ component when considering only linear segment configurations.

The term $\partial V/\partial z$ will be dropped immediately since it vanishes for adjacent segments and the contributions from the gradient of the potential V due to end charges for the end segments may be assumed negligible [13]. Note that although this expression for E_z is relatively simple, this closed form expression is rigorous even in the near-zone.

The complex coefficients A and B in the expression for I(z) (see Equation 20) can be solved in terms of the end currents I_1 and I_2. The resulting equation for I(z) is

$$I(z) = [I_1 \sin k(z_2 - z) + I_2 \sin k(z - z_1)] / \sin kd \qquad (22)$$

where d as indicated in Figure 3 is the length of the segment.

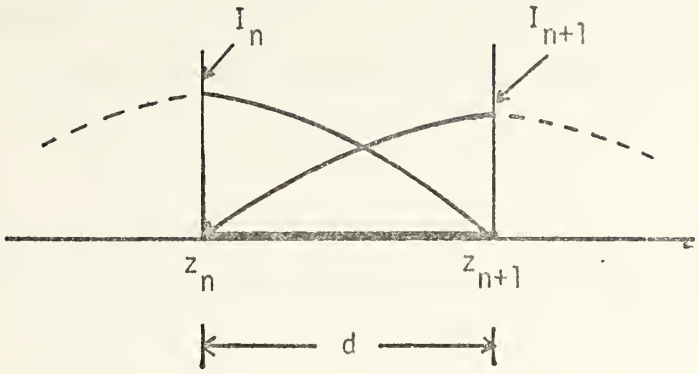

FIGURE 3. Piecewise-sinusoidal current distribution on an antenna segment.

Figure 3 illustrates the current distribution expressed in Equation (22). It is clear that from Equation (22) I_1' and I_2' may also be expressed in terms of I_1 and I_2. Since

$$I'(z) = [-kI_1 \cos k(z_2 - z) + kI_2 \cos k(z - z_1)] / \sin kd \qquad (23)$$

it follows that

$$I_1' = k(I_2 - I_1 \cos kd) / \sin kd \qquad (24A)$$

$$I_2' = k(I_2 \cos kd - I_1) / \sin kd \quad . \qquad (24B)$$

Note that from Equations (21) and (24) the electric field intensity of the sinusoidal electric line source may be expressed entirely in terms of the geometry of the observation point and the end currents I_1 and I_2.

D. EXPANSION OF THE CURRENT DISTRIBUTION

The forms of the current distributions on both of the filamentary dipoles is piecewise-sinusoidal. The current on each segment of each dipole can be described by the sinusoidal functions given in Equation (22). Because the components of the electric field intensity of such an element are known, both terms within the integral of Equation (19) exist as closed form expressions.

The following piecewise-sinusoidal distribution has been employed by Richmond [15]:

$$\bar{J}_s = \frac{1}{2\pi a} I(\ell) = \frac{1}{2\pi a} \sum_{n=1}^{N-1} I_n \hat{\tau}_n P_n(\ell) \frac{\sin k(\ell - \ell_{n-1})}{\sin kd} + \hat{\tau}_{n+1} P_{n+1}(\ell) \frac{\sin k(\ell_{n+1} - \ell)}{\sin kd} \quad (25)$$

or

$$\bar{J}_s = \frac{1}{2\pi a} \sum_{n=1}^{N-1} I_n \bar{G}_n \quad (26)$$

with $I_n = I(\ell_n)$ and d the length of the segment. $P_n(\ell)$ is a unit pulse, nonzero only on segment n; $\hat{\tau}_n$ is a unit vector pointing in the direction of ℓ from one endpoint of segment n to the other. The vector functions $\bar{G}_n$ are known as basis functions, expansion functions or dipole modes. The mode currents go to zero at the endpoints of the dipoles, as depicted in Figure 4.

It is advantageous to have a symmetric impedance matrix Z_{mn} (to be defined later). Furthermore, the test sources should be chosen to yield a well-conditioned system of linear equations for the subsequent inversion process. For these reasons and to obtain a closed form expression for the integral of Equation (19), the expansion function for the test source $\bar{G}_m$ will be of the same form as the basis function for the original dipole's current distribution $\bar{G}_n$.

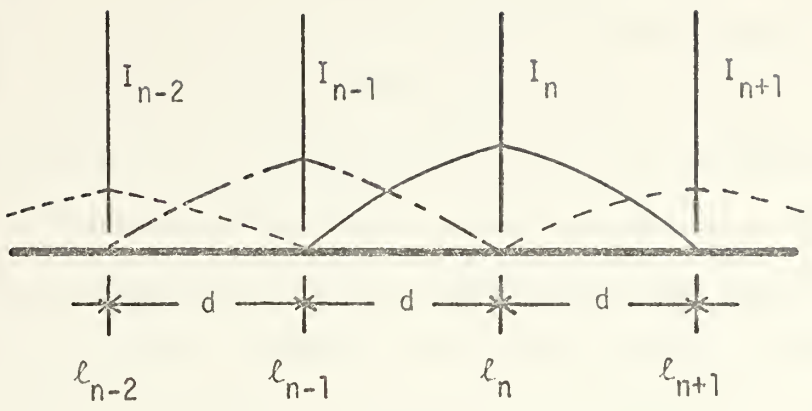

FIGURE 4. Basis functions ($\overline{G}_n$) representing the assumed current distributions on a linear filamentary antenna.

With the piecewise-sinusoidal current distribution employed for each segment of the antenna, then from Equation (22) the current on any given segment can be considered the sum of two sinusoidal currents, each of which vanishes at one or the other end of the segment. This may be visualized with the aid of Figure 4. One can see how the equivalent surface distribution is treated as a collection of (N-1) overlapping tubular dipole current densities on an antenna consisting of N segments. The nth dipole has terminal current I_n at the nth junction with the current vanishing at the far ends of the two segments forming the nth junction.

The solution for the unknown complex terminal currents $\{I_n\}$ proceeds by introducing a set of (N-1) filamentary dipoles each having piecewise-sinusoidal currents and being located along the axis of the original antenna. No generality is lost by assuming each test dipole has unit terminal current. Reciprocity is enforced successively between each test dipole and all the tubular surface dipoles in turn. The "zero reaction condition" yields the following equation for the mth test dipole and the nth surface-current dipole (refer to Equation (15)):

$$\iint_{S_n} \bar{M}_n \cdot \bar{H}_m \, ds_n = \iint_{S_n} \bar{J}_n \cdot \bar{E}_m \, ds_n \quad . \qquad (27)$$

The left-hand side of Equation (27) is nonzero only when n = m. This is the result of the tangential component

of the electric field on the surface of the original source being zero except at the delta gap. $\bar{M}_n$ which equals $\bar{E}_n \times \hat{n}$ is therefore also zero unless the mth test dipole is co-located with the nth original dipole. Expressed mathematically:

$$\iint_{S_n} \bar{M}_n \cdot \bar{H}_m \, ds_n = -V_n \int_{\ell_n} \bar{H}_m \, d\ell_n \, \delta_{mn} = -V_n \, \bar{I}_m \, \delta_{mn} \, . \tag{28}$$

The right-hand side of Equation (27) can be simplified by carrying out the circumferential integration of $\bar{J}_n \cdot \bar{E}_m$. Again this is equivalent to replacing the tubular distribution with filamentary segments for calculating reaction:

$$\iint_{S_n} \bar{J}_n \cdot \bar{E}_m \, ds_n = \int_{\ell_n} \bar{I}_n(\ell_n) \cdot \bar{E}_m \, d\ell_n \, . \tag{29}$$

Equating Equations (28) and (29) one obtains

$$-V_n \, \bar{I}_m \, \delta_{mn} = \int_{\ell_n} \bar{I}_n(\ell_n) \cdot \bar{E}_m \, d\ell_n \, . \tag{30}$$

Assuming unit amplitude for the test current and noting that upon co-locating m = n,

$$V_m \, \delta_{mn} = - \int_{\tau_n} \bar{I}_n(\tau_n) \cdot \bar{E}_m \, d\tau_n \tag{31}$$

The integration is carried out on τ_n, the coordinate along the arms of the nth surface dipole filaments. The

symbol δ_{mn} is the standard Kronecker delta, defined by the relations:

$$\delta_{mn} = 0 \qquad m \neq n$$

$$\neq 0 \qquad m = n \quad . \tag{32}$$

Equation (31) forms the basis of the multi-segment reaction matching technique.

E. MATRIX EQUATION FORMULATION

Substitute the assumed form of $\bar{I}_n(\tau_n)$ (refer to Figure 4) namely

$$\bar{I}_n(\tau_n) = I_n \left[\hat{\tau}_n \, P_n(\ell) \, \frac{\sin k(\ell - \ell_{n-1})}{\sin kd} + \hat{\tau}_{n+1} \, P_{n+1}(\ell) \, \frac{\sin k(\ell_{n+1} - \ell)}{\sin kd} \right] \tag{33}$$

into Equation (31) and define a mutual impedance term as

$$Z_{mn} = -\int_{\ell_{n-1}}^{\ell_n} \frac{\sin k(\ell - \ell_{n-1})}{\sin kd} \hat{\tau}_n \cdot \bar{E}_m \, d\ell$$

$$- \int_{\ell_n}^{\ell_{n+1}} \frac{\sin k(\ell_{n+1} - \ell)}{\sin kd} \hat{\tau}_{n+1} \cdot \bar{E}_m \, d\ell. \tag{34}$$

The dummy variable ℓ is the coordinate along the particular segment, the other variables are defined as in Equation (25).

$\bar{E}_m$ as before, is the free space electric field intensity radiated by the mth test dipole with piecewise-sinusoidal current, specifically for the mth test dipole composed of a lower segment ML and an upper segment MU, the z component of the electric field is

$$\bar{E}_m = \frac{\hat{z}}{4\pi j\omega\epsilon}\left\{ \frac{I'_{1ML}\, e^{-jkR_{1ML}}}{R_{1ML}} - \frac{I'_{2ML}\, e^{-jkR_{2ML}}}{R_{2ML}} + \frac{I'_{1MU}\, e^{-jkR_{1MU}}}{R_{1MU}} - \frac{I'_{2MU}\, e^{-jkR_{2MU}}}{R_{2MU}} \right\} \qquad (35)$$

where as depicted in Figure 5, $I'_{1ML} = I'_1$ of segment ML, $I'_{1MU} = I_1$ of segment MU, $R_{1ML} = R_1$ of segment ML, $R_{1MU} = R_1$ of segment MU etc...

Figure 5 is merely an extension of the single segment with piecewise-sinusoidal currents of Figure 2 to a dipole composed of two such segments.

Equation (31) may now be written

$$V_m \delta_{mn} = Z_{mn} I_n \quad , \qquad (36)$$

where I_n is the complex terminal current at the nth junction. The calculation of the reaction between the mth test dipole and the entire equivalent surface current density, consisting of N-1 overlapping surface dipoles, yields the following relation:

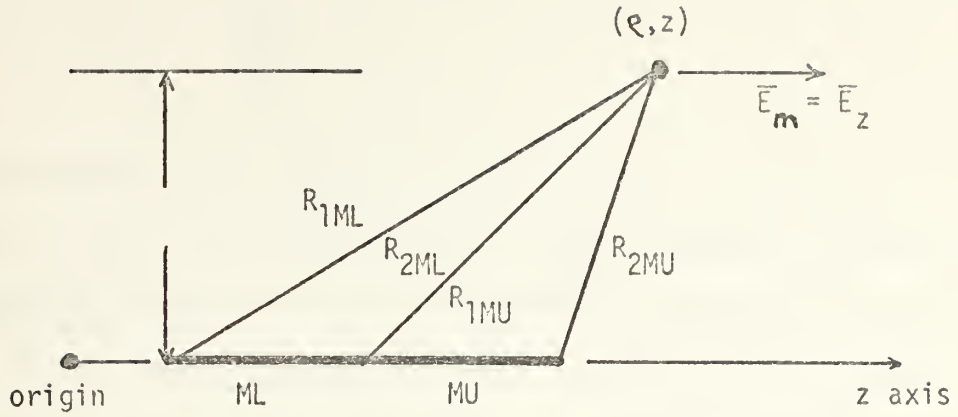

FIGURE 5. The m^{th} test dipole, composed of a lower segment ML and an upper segment MU

$$V_m = \sum_{n=1}^{N-1} Z_{mn} I_n \quad . \tag{37}$$

Equation (37) represents one linear equation out of a system of (N - 1) equations that are obtained by successively enforcing reciprocity (or calculating reaction) between the (N - 1) surface dipoles and each of the (N - 1) axial test dipoles in turn. The test is performed in turn between each of the axial dipoles and the tubular dipoles yielding a system of linear equations that can be described by the matrix relation

$$[Z_{mn}] [I_n] = [V_m] \quad , \tag{38}$$

which is of the same form as Equation (37), except that Z_{mn} is now a square (N - 1) X (N - 1) matrix and V_m is a column vector. This set of equations can be solved for the unknown junction current coefficients $\{I_n\}$ after a known voltage source is placed at the actual feed junctions and the voltage of the other junctions are set to zero.

The coefficients I_n of Equation (38) can be solved for by several techniques. Crout published a paper [7] in which he discusses a method for evaluating determinants and solving systems of linear equations with complex coefficients. In the case of well conditioned matrices the impedance matrix can be merely inverted and multiplied

by the voltage matrix to yield the terminal current coefficients:

$$[I_n] = [Z_{mn}]^{-1} [V_m] \tag{39}$$

Equation (39) may be written simply as

$$[I] = [Z]^{-1} [V] \tag{40A}$$

or equivalently:

$$[I] = [Y] [V] \quad , \tag{40B}$$

where

$$[Y] = [Z]^{-1} \quad .$$

The complex current coefficients I_n that are determined from Equation (38) are used to establish the current distribution found from Equation (26). Once the current distribution is known, parameters of interest such as field patterns, input admittances, etc., can be calculated by numerically evaluating the appropriate formulas.

A wire antenna is obtained when the wire is excited by a voltage source at one or more points along its length. For an antenna excited at the nth junction, the applied voltage matrix of Equation (40) is

$$[V_n] = \begin{bmatrix} 0 \\ \cdot \\ \cdot \\ V_n \\ \cdot \\ \cdot \\ \cdot \\ 0 \end{bmatrix} \tag{41}$$

that is, all elements of the voltage matrix are zero except the nth, which is equal to the source voltage. The current distribution is established by Equation (40) which for the $[V_n]$ of Equation (41) becomes

$$[I] = V_n \begin{bmatrix} Y_{1n} \\ Y_{2n} \\ Y_{3n} \\ \cdot \\ \cdot \\ \cdot \\ Y_{mn} \end{bmatrix} . \tag{42}$$

Note that the nth column of the admittance matrix gives the current distribution for a unit voltage source applied to the nth junction. Inversion of the impedance matrix therefore gives simultaneously the current distributions when the antenna is excited at any arbitrary junction along its length. For the case where only one junction is excited with a voltage V_i, the input admittance is given directly by the feed junction current I_i as

$$Y_{IN} = \frac{I_i}{V_i} \quad . \tag{43}$$

F. SOLUTION TECHNIQUES

As mentioned previously, integrals of the form of Equation (34) can be obtained in closed form for coplanar segments. In the case of non-coplanar segments, the integrals must be calculated by numerical methods, for example, Simpson's rule or Gaussian quadrature.

Upon a careful examination of Equations (34) and (35) it should be ovbious that the integral of Equation (35) may be expressed in closed form with the relationship [16] that follows:

$$z_m \int_{r_1}^{r_2} \frac{\exp(\mp jr)\ \exp(-jR_m)}{rR_m}\, dr = [\exp(-jz_m)\ E(R_m - z_m \mp r) - \exp(jz_m)\ E(R_m + z_m \mp r)]_{r=r_1}^{r=r_2} \tag{44}$$

where

$$Ci(x) = \gamma + Ln(x) + \int_0^x \frac{\cos(t) - 1}{t}\, dt \tag{45A}$$

$$Si(x) = \int_0^x \frac{\sin(t)}{t}\, dt - \frac{\pi}{2} \quad . \tag{45B}$$

Utilizing the relationship in Equation (44), Richmond and Geary published a paper [16] that developed a closed form expression for the mutual impedance between coplanar skew dipoles. However, for this antenna problem, all of the reactions will be performed between parallel dipoles. A more useful closed form expression for the problem consisting of entirely parallel dipoles was presented by H. E. King [10]. The complete expression with its derivation may be found in Appendix A and B. Even though these closed form expressions are not particularly simple, they do involve only sine and cosine integrals which have polynomial algorithms; hence Z_{mn} in this form is more efficient than "brute-force" integration.

Leonard Tsai [21] formally portrayed PSRMT as a particular application of Galerkin's method. Consider again the operator equation

$$L(\overline{f}) = \overline{g} \tag{46}$$

where $\overline{f}$, the given operator, is specifically the unknown current distribution on a filamentary dipole and the operator L yields the fields $\overline{g}$ of a distance "a" away (on the original dipole). Expanding $\overline{f}$ into a linear combination of basis functions:

$$\overline{f}_n = \sum_n c_n \overline{f}_n \tag{47}$$

and enforcing Galerkin's method directly:

$$\sum_n c_n \langle L\bar{f}_n, \bar{f}_m \rangle = \langle \bar{g}, \bar{f}_m \rangle \quad . \tag{48}$$

Here the $\bar{f}_m$ would describe the weighting functions corresponding to the "test dipoles" which is using the same expansion functions as the "original dipoles", both subdomain piecewise-sinusoidal pulses. The inner product of the left-hand side of Equation (48) corresponds directly to the integral of Equation (31):

$$\int_n \bar{I}_n \cdot \bar{E}_m \, d\tau_n \tag{49}$$

used in the reaction matching technique. Note also that $\langle g, f_m \rangle = V_m$ which is nonzero only at voltage sources. This follows from the "zero reaction condition". Thus the procedures of PSRMT are those employed by a direct application of Galerkin's method.

V. DISCUSSION OF NUMERICAL TECHNIQUES AND COMPUTER PROGRAM

Evaluation of the integrals in Equation (34) may be accomplished by any one of several numerical integration techniques such as Romberg, Weddle, Gaussian Quadrature, etc., as well as by the closed form expression developed in Appendix A. For most integrals, no representation in terms of elementary functions is possible, and approximation becomes necessary. Most numerical techniques are successfully based upon some type of polynomial approximation: trapezoidal rule, Simpson's rule, Romberg's method, etc.. Unfortunately, these techniques have the usual error sources such as truncation, but perhaps more interestingly they are harassed with the question of convergence. The question is whether as continually higher degree polynomials are used or as continually smaller intervals between data points are used, a sequence of approximations is produced for which the limit of the truncation error is zero. As may be guessed, the smaller the interval h is made, the more computation time required and the greater the rounding off error becomes. In other words, accuracy is limited for any given method by algorithm errors that ultimately obscure convergence.

It is found in practice that decreasing the interval between sampling points below a certain level leads to larger errors rather than smaller. This necessitates

experimentation of the various parameters available in the technique in order to establish a trend (if one exists) that gives acceptable results. Unfortunately this requires an assumed correct solution in order to evaluate the performance of the integration on a supposedly unknown integral.

Table 1 illustrates how the value for input admittance of a half-wave dipole varies as a function of the number of antenna segments and the order of the Gaussian Quadrature used in evaluating the integral of Equation (34). Table 2 is a similar portrayal of a full-wave antenna.

The norm for Table 1 and 2 was chosen to be the value of input admittance given by King [11]. Table 1 shows no convergence tendency whatsoever, while Table 2 indicates that a lower degree polynomial may be used in evaluating Z_{mn} if the antenna is divided into more segments. The apparent discrepancy between Table 1 and 2 is probably explained by the difference in the actual current distributions on the two antennas. It is clear that the problem is multi-faceted.

This convergence problem is not exclusive to the Gaussian Quadrature technique. In fact, all of the numerical techniques have some troublesome parameter analysis involved in order to effectively use them. But a far more important and exciting reason to avoid their use is that of efficiency. The closed form expression involves only the evaluation of the sine and cosine integrals which have

Number of Segments	ORDER OF GAUSSIAN QUADRATURE						
	3	4	5	6	7	8	9
4	7.5	3.5	2	.5	0	.5	1
6	7.5	4.0	2.5	2	1.5	1.5	1
8		4.5	3	3	2.5	2.5	2.5
10		4.5	3.5	3.5	3	3	3.5
12		4.5	4	4	3.5	4	4
14			4.5	5	4	4.5	4.5
16			4.5	5.5	4.5	5	5

TABLE 1. Convergence analysis for the input admittance of a half-wave dipole. The numbers respresent percent variation from the King-Middleton standard of Y= 10.8 mmho's. (Percentages expressed to the nearest .5%)

Number of Segments	ORDER OF GAUSSIAN QUADRATURE							
	2	3	4	5	6	7	8	9
4					20	5	4.5	11
6				25	10	1	8	12
8				18	3.5	5	9.5	12
10			30	11	.5	6.5	10	
12			25	6	3	7.5	10	
14		50	20	3	4	7.5		
16		45	15	1	4.5	6.5		
18	105	35	11	.5	5.5			
20	95	30	8	1.5	7			
22	85	28	6	2				
24	80	24	4.5	3				

TABLE 2. Convergence analysis for the input admittance of a full-wave dipole. The numbers represent percent variation from the King-Middleton standard of Y = -90 mmho's. (Percentages less than 20 expressed to the nearest .5%)

simple algorithms. Unfortunately the closed form solution is valid in general for skewed coplanar dipoles only, therefore, numerical integration would be required for non-coplanar elements. The same antenna problem (if coplanar) may be solved by the closed form technique in a fraction of the time that numerical methods require.

The computer program listed in Appendix B calls upon subroutine CZMN2 for the evaluation of the impedance matrix. It is here that the method of solution may be chosen. If the closed-form route is decided upon, CZMN1 (which is also listed) is used to evaluate Z_{mn}.

VI. ANALYSIS OF RESULTS

A. CONVERGENCE CHECK

Figures 6 and 7 illustrate the accuracy and efficiency of PSRMT. Leonard Tsai [21] used similar figures (the solution labeled "Richmond's Reaction") to show the comparative rate of convergence of PSRMT to that of point matching with triangular pulses. Note that reaction matching required only six segments while for the same accuracy point matching required five times as many segments. Superimposed on Tsai's comparison are those points generated by the closed form expressions of Equation (72) of Appendix B.

Figures 8 and 9 illustrate the efficiency of PSRMT. In Figure 8, as more and more flat pulses are employed in Galerkin's method the more the solution corresponds to that of PSRMT with only six segments. Figure 9 shows how rapidly PSRMT relates to the moment method employing piecewise-sinusoidal basis functions.

Figure 10 exemplifies the convergence of PSRMT itself. The comparison is drawn between PSRMT and Hallen's equation employing piecewise-sinusoidal basis functions. 16 segments do an admirable job in relating to this half-wave dipole. This is sufficiently true under certain conditions (as will be shown) to warrant a rule of thumb: use 32 segments per wavelength.

Figure 11 is a plot of conductance versus susceptance for thin cylindrical dipoles with radius $a/\lambda = .001588$. The locus spirals in as the length of the dipole increases. Note that for small lengths the 8 segmented solution deviates from the accepted King-Middleton value of admittance. Many of the plots to follow will use King-Middleton values for comparison, which were taken from tables published by R. W. P. King [11]. In the evaluation of the admittance, the King-Middleton procedure was again used (two iterations and an empirical normalization were also employed). Figure 11 indicates the advantage of taking 32 segments per wavelength.

Figure 12 is the same type as Figure 11 but the radius has been increased to $.00635\lambda$. It is evident that for short dipoles with large radii, the length to radius ratio for each segment exceeds the thin-wire approximation. That is why that as the length of the antenna is increased in Figure 12, the solution becomes more convergent.

Figures 13 and 14 portray the convergence trends of the Weddle numerical integration technique on a half-wave dipole. As indicated in Figure 13, the solution varies only slightly with a change in the number of integration points used in the integration. However, the input admittance approaches the King-Middleton solution most nearly when the number of integration points equals 29. Figure 14 shows the change in current distribution as the number of antenna segments change (with the number of integration points equal to 29).

Again the input admittance approaches the King-Middleton solution as the number of segments increase. These particular trends are valid only for this half-wave dipole of radius $a/\lambda = .001588$. Other geometries must be considered on a one to one basis due to the behavior of Weddle's technique on the integral of Equation (34).

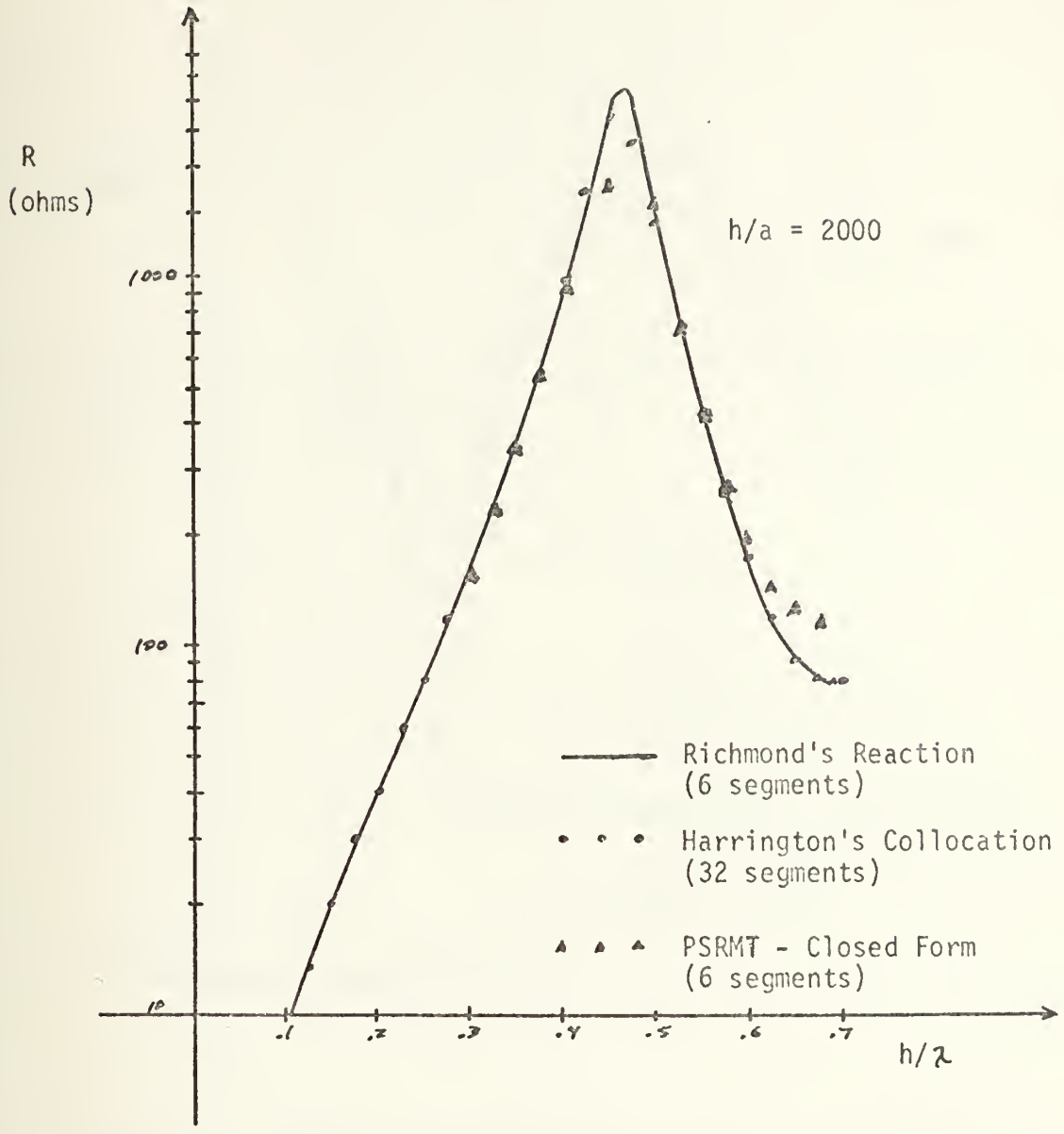

FIGURE 6. Input resistance versus h/λ for a cylindrical wire antenna with radius a and total length L = 2h.

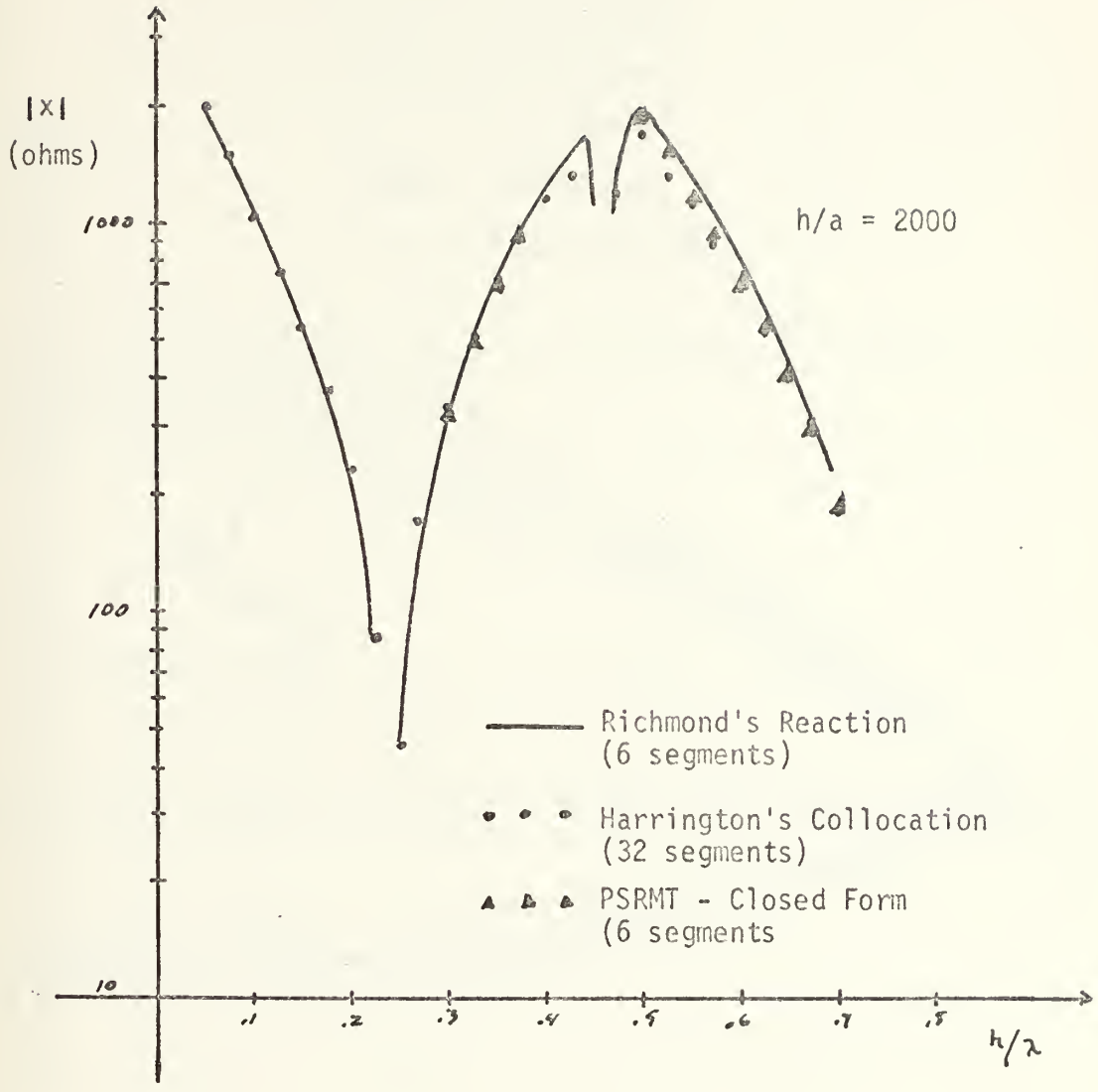

FIGURE 7. Input reactance versus h/λ for a cylindrical wire antenna with radius a and total length L = 2h.

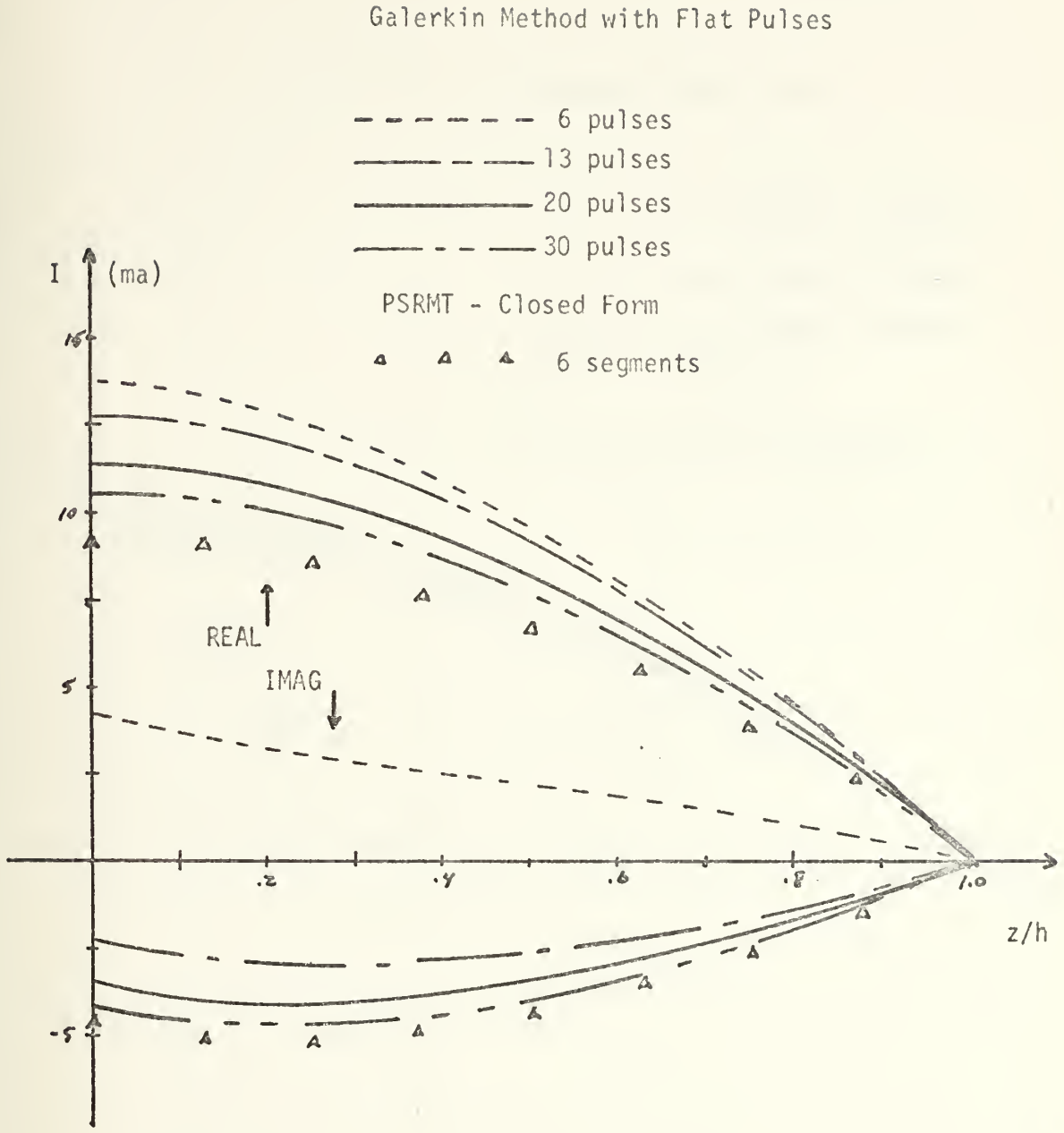

FIGURE 8. Current distribution on a half-wave dipole with radius $a/\lambda = .001588$.
(Galerkin Method with flat pulses)

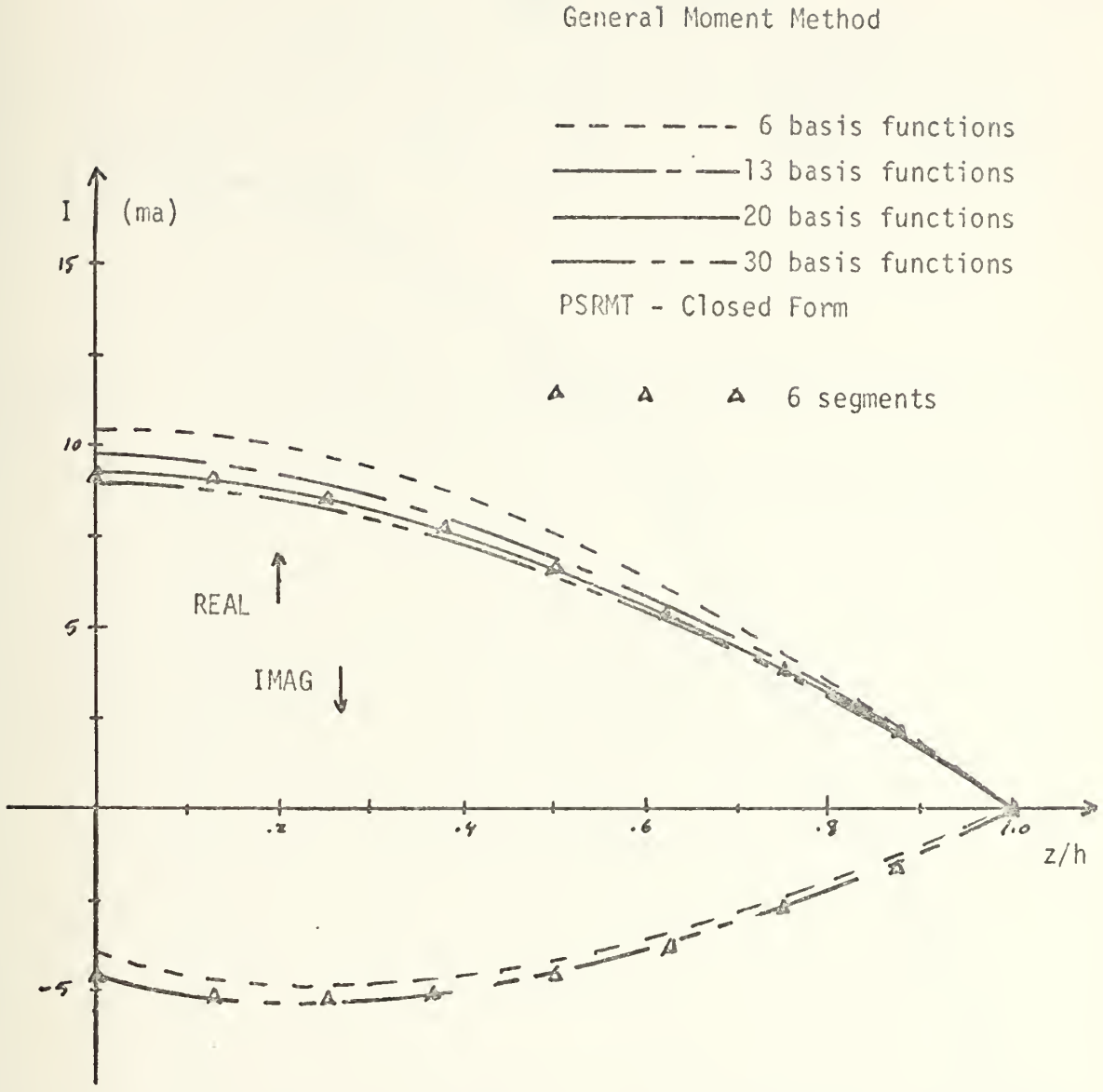

FIGURE 9. Current distribution on a half-wave dipole with radius $h/\lambda = .001588$.
(General moment method — piecewise-sinusoidal pulses)

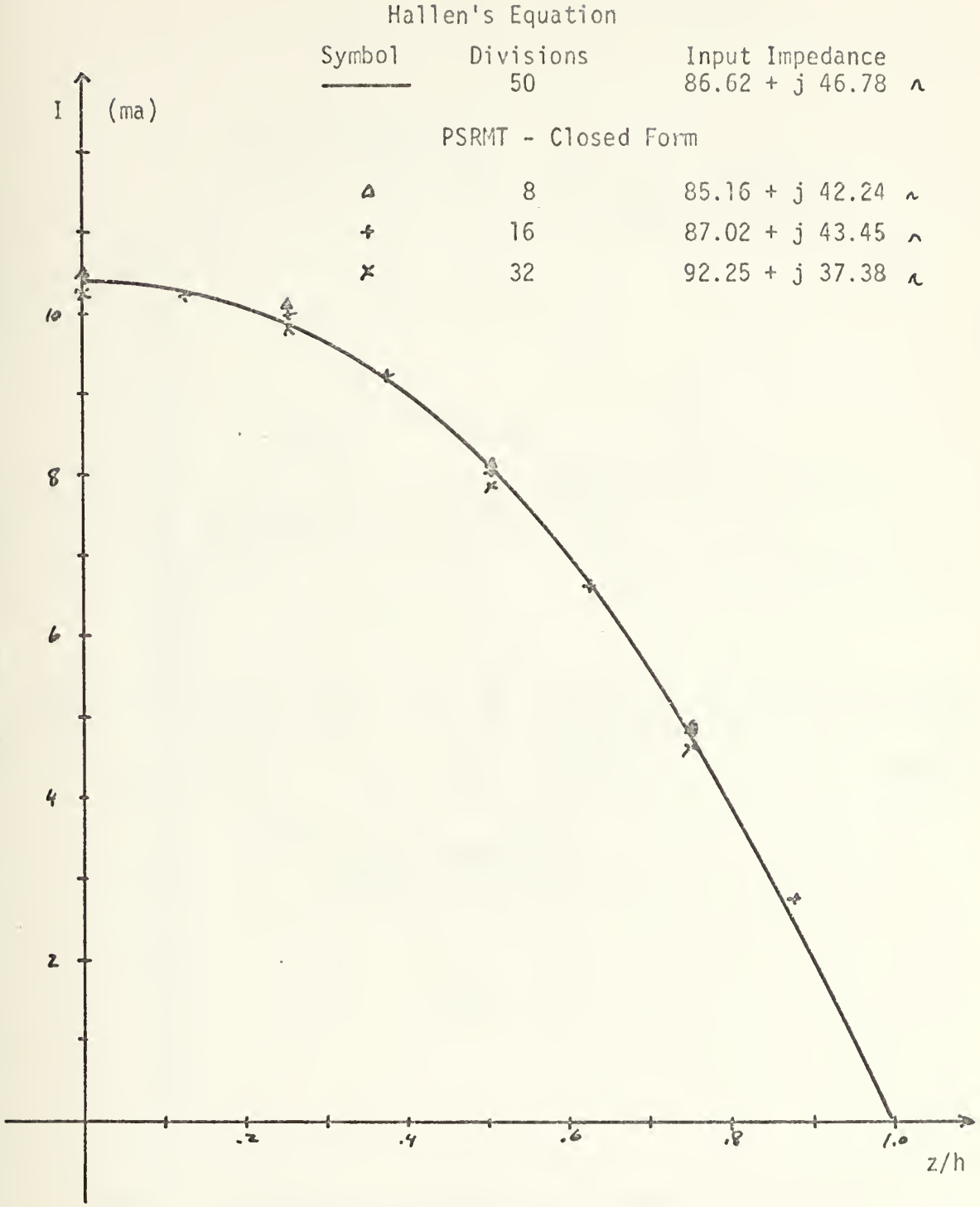

FIGURE 10. Current distribution on a half-wave dipole with radius $a/\lambda = .001$.
(Hallen's Equation - piecewise - sinusoidal - basis functions)

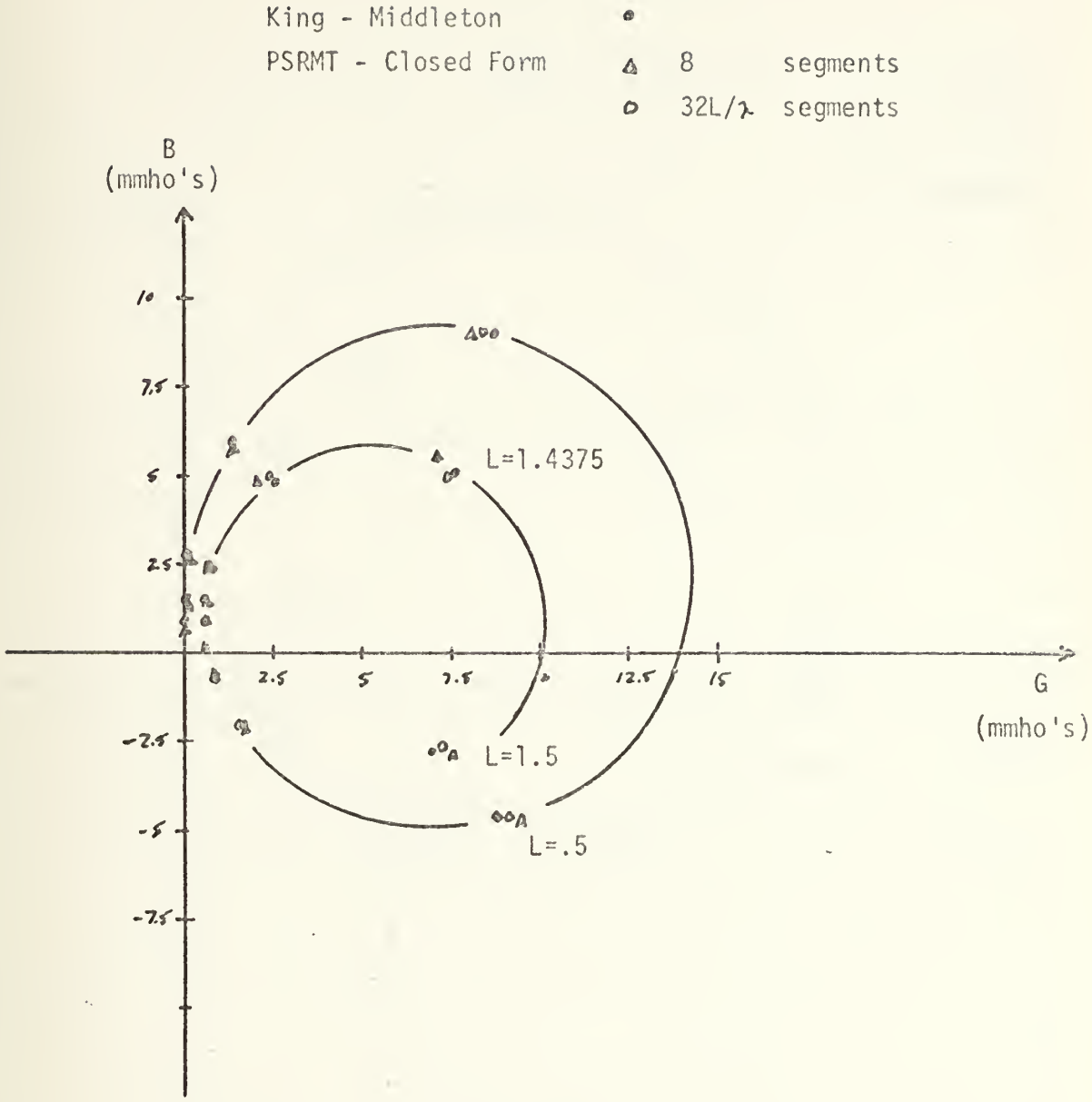

FIGURE 11. Admittance curve for thin-cylindrical dipoles with radius $a/\lambda = .001588$.

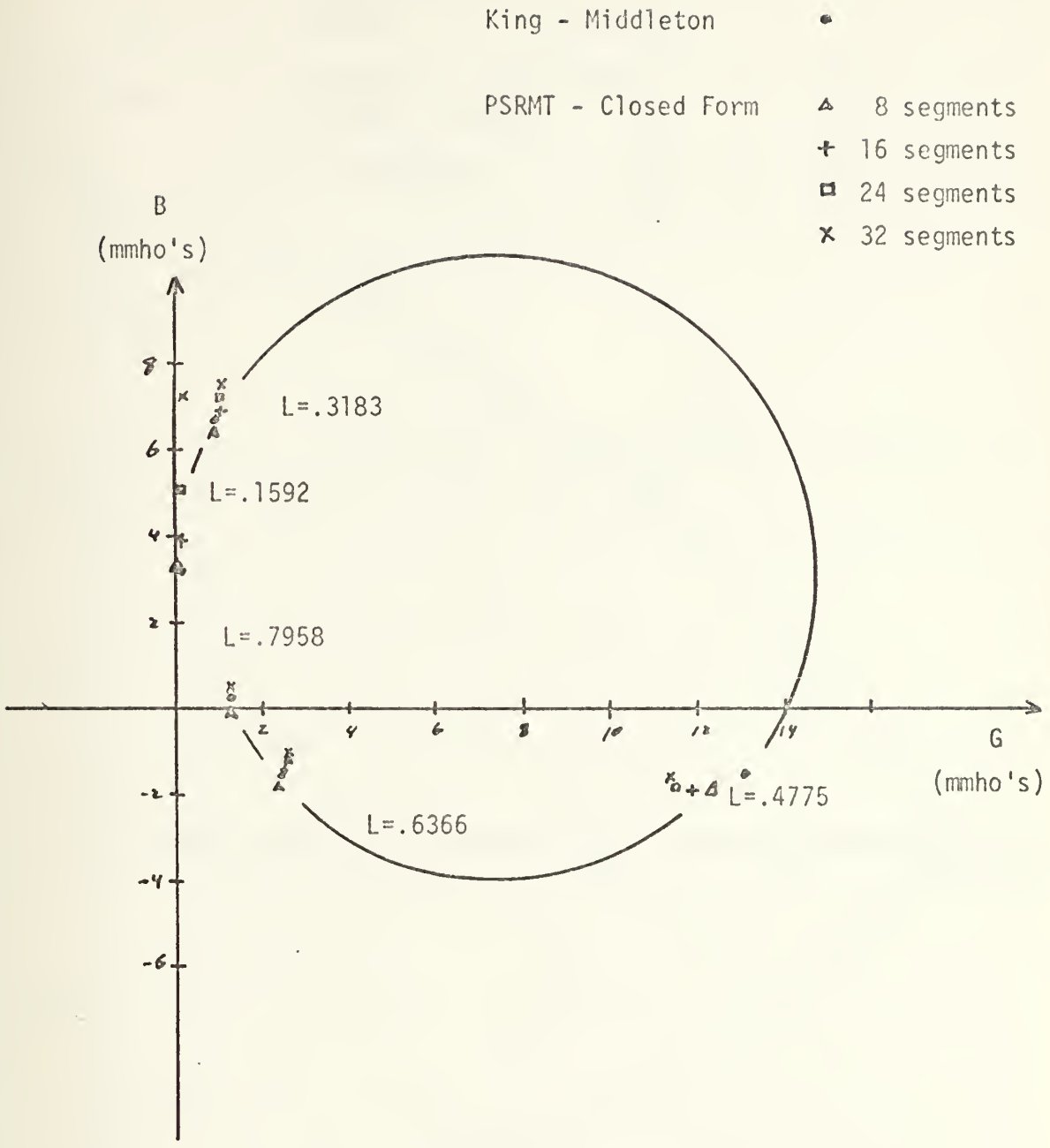

FIGURE 12. Admittance curve for thin cylindrical dipoles with radius $a/\lambda = .00635$.

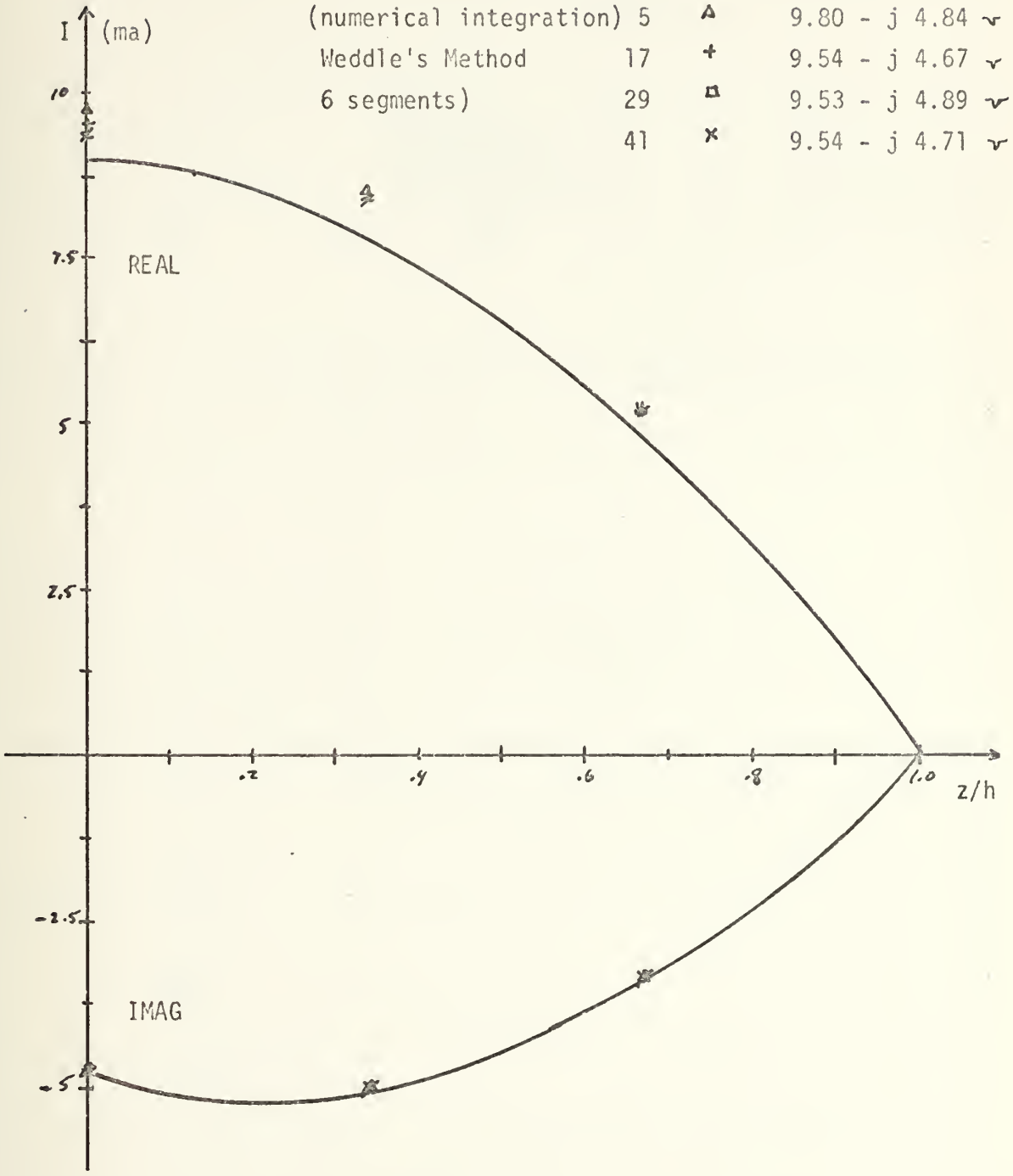

FIGURE 13. Current distribution on a half-wave dipole with radius a/λ = .001588 (convergence check on the number of integration points used in Weddle's technique)

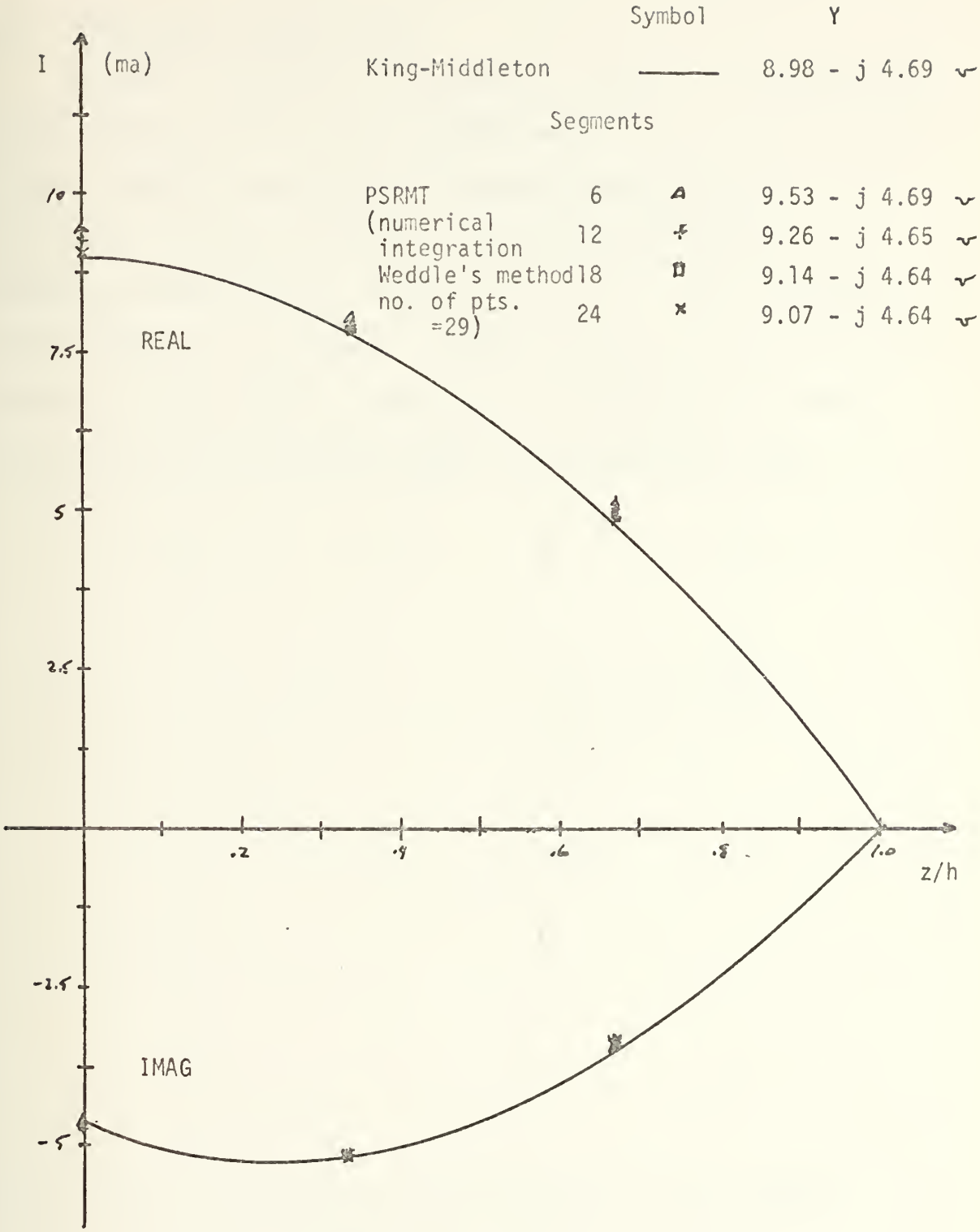

FIGURE 14. Current distribution on a half-wave dipole with radius $a/\lambda = .001588$.
(convergence check on the number of segments used in Weddle's technique)

B. ADMITTANCE CORRELATION

Figures 15 through 18 attempt to typify the admittance correlation between the King-Middleton solution and various PSRMT solution techniques. Figure 15 and 16 depict the solution by Weddle's method and the Gaussian Quadrature method, respectively. Figures 17 and 18 can be compared with Figure 11 to show the effect of changing the dipole's radius. The effect is negligible as long as the length to radius ratio of each segment is maintained large.

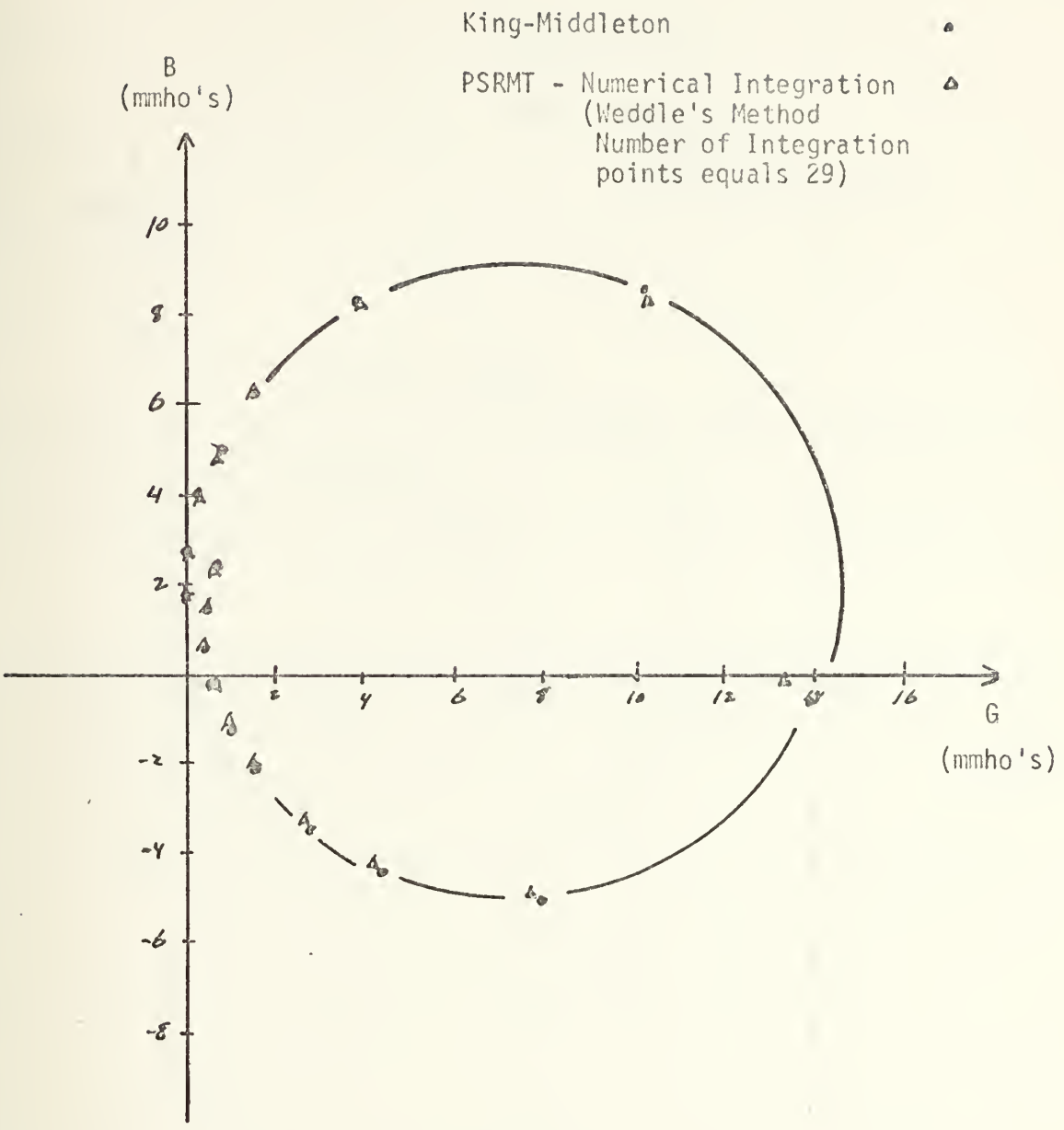

FIGURE 15. Admittance correlation for thin cylindrical dipoles with radius $a/\lambda = .001588$. (32 L/λ segments)

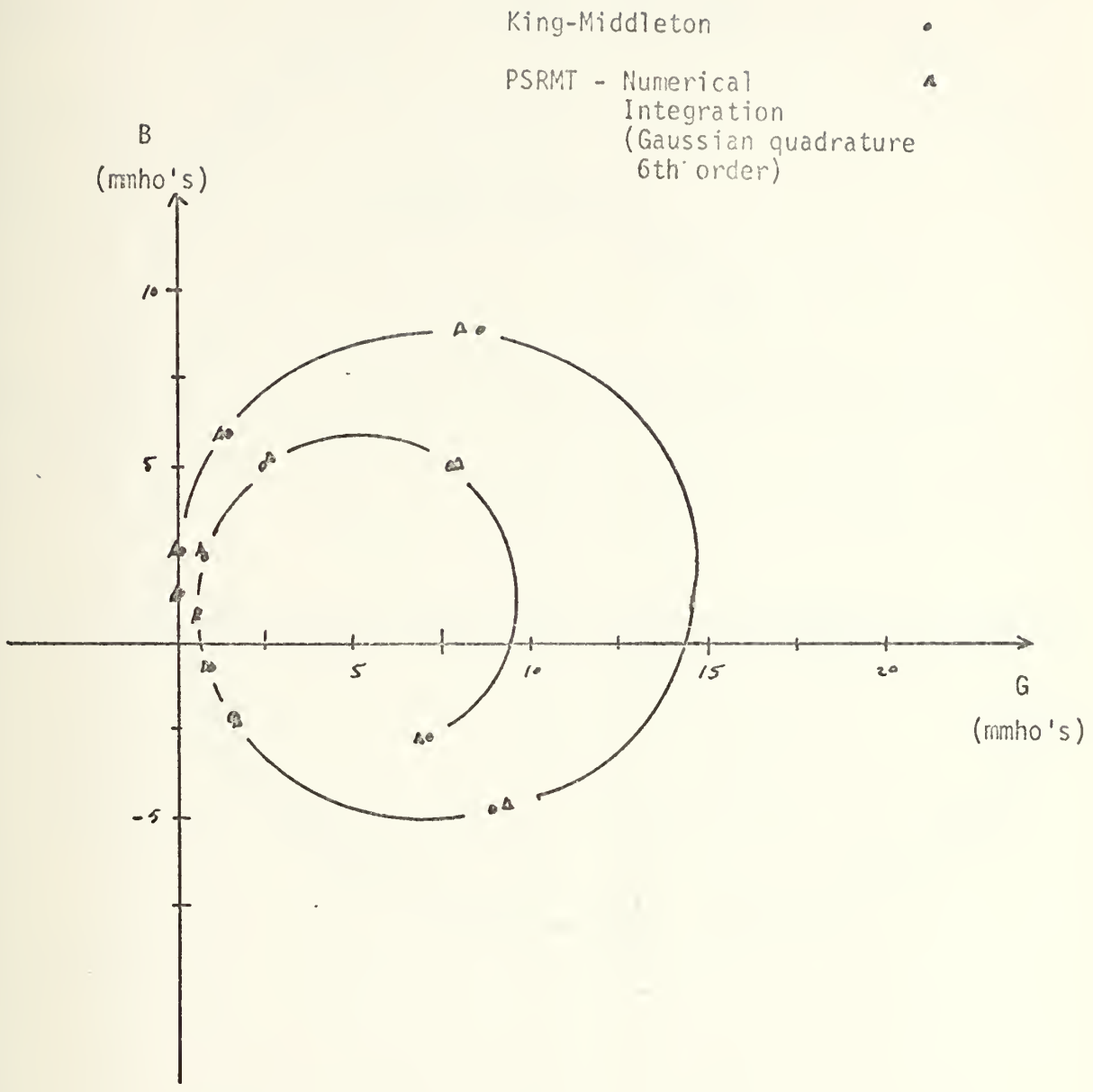

FIGURE 16. Admittance correlation for thin cylindrical dipoles with radius $a/\lambda = .001588$. (32 L/λ segments)

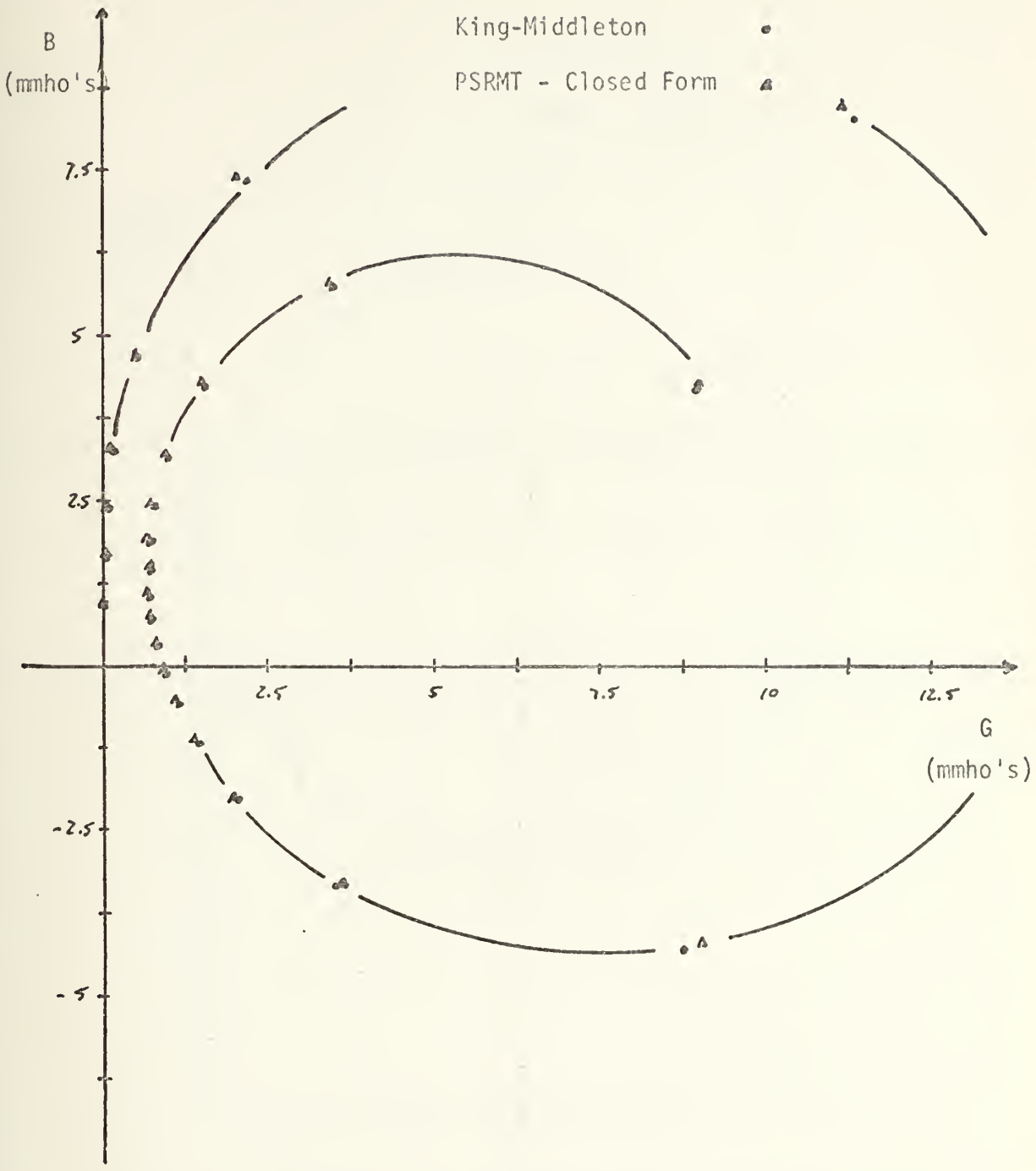

FIGURE 17. Admittance correlation for thin cylindrical dipoles with radius $a/\lambda = .003175$. (32 L/λ segments)

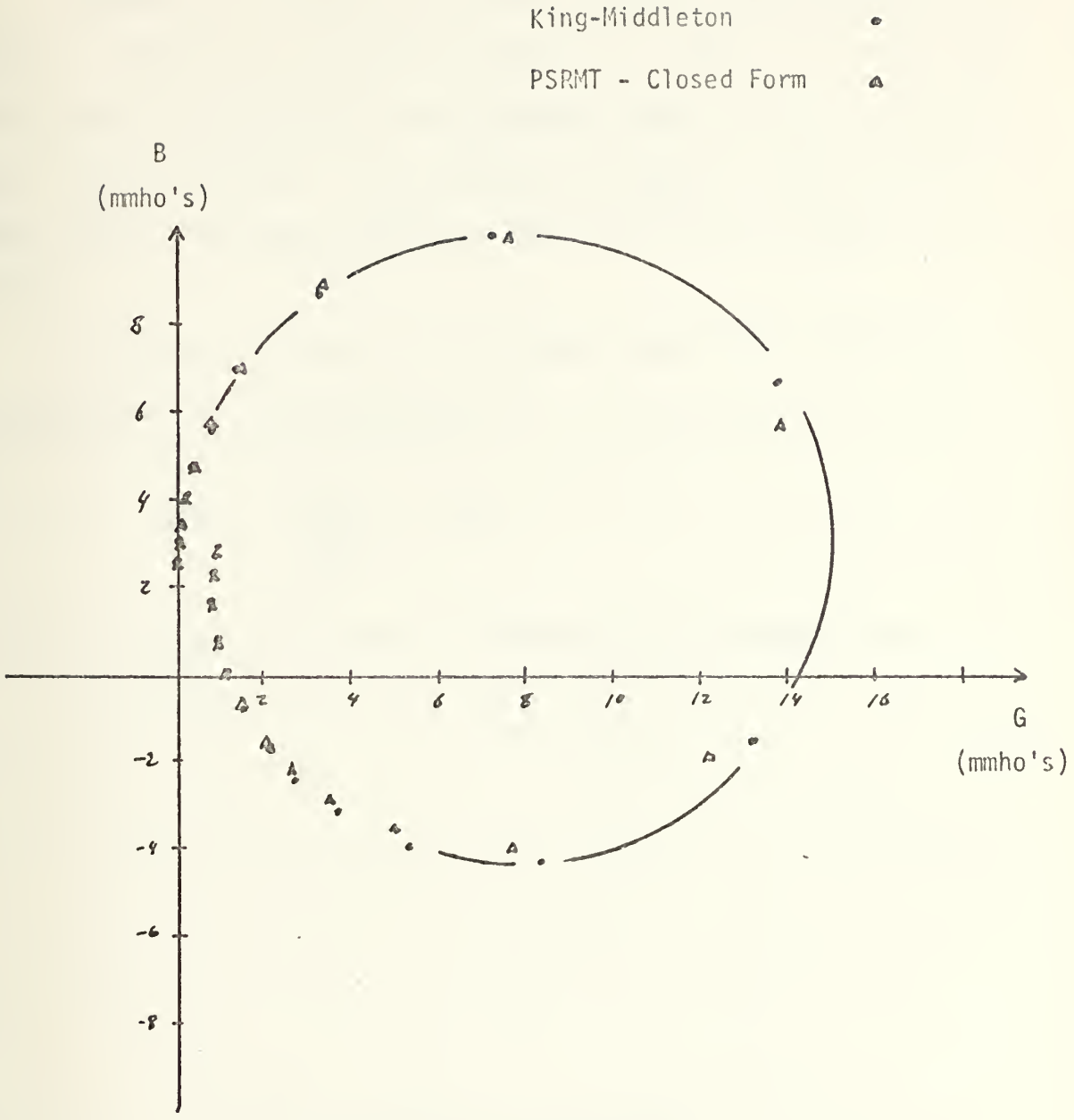

FIGURE 19. Admittance correlation for thin cylindrical dipoles with radius a/λ = .004763. (32 L/λ segments)

C. CURRENT DISTRIBUTIONS

Figures 19 through 25 present current distributions on dipole antennas of various lengths and radii. On each set of curves is indicated the expansion set used to represent the unknown current. The number of segments employed in the PSRMT technique was based upon the rule of thumb $32\ L/\lambda$.

In Figures 24 and 25, the power series [2] used as a comparison may be expressed as

$$I(z) = \sum_{n=1}^{5} C_n\, z^{n-1} \quad ,$$

where the C_n's are complex constants to be determined.

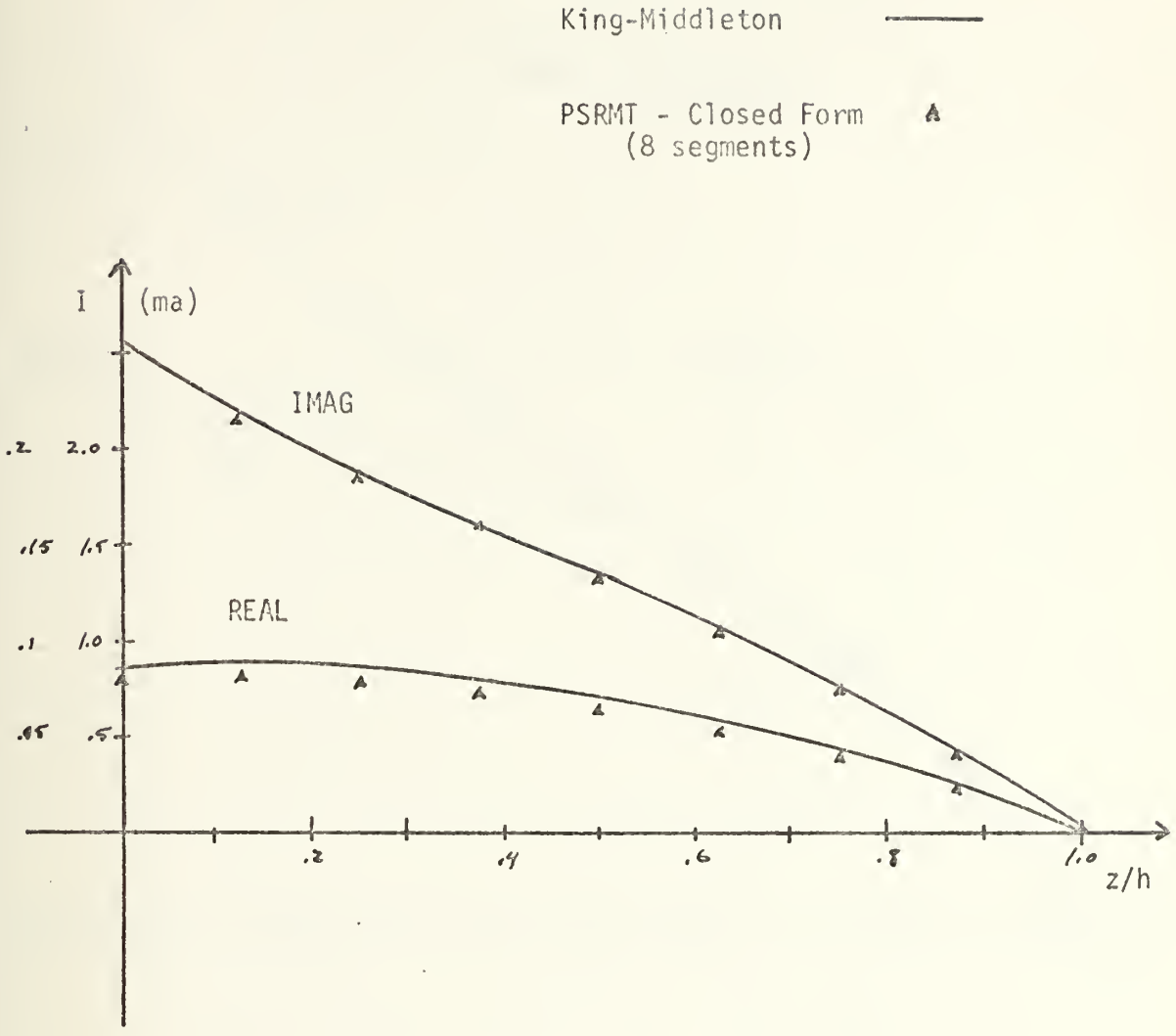

FIGURE 19. Current distribution on a quarter-wave dipole with radius $a/\lambda = .001589$.

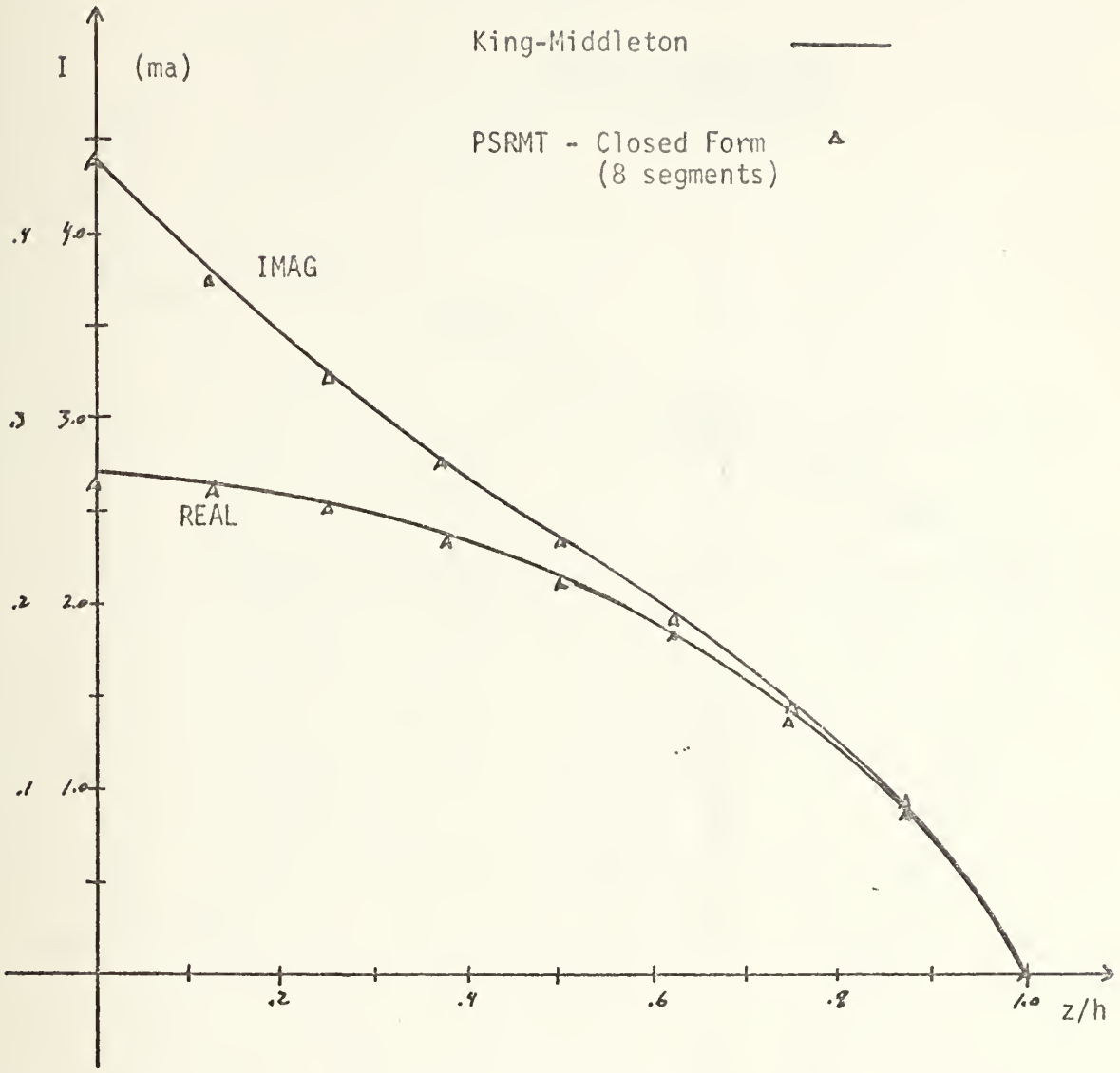

FIGURE 20. Current distribution on a quarter-wave dipole with radius $a/\lambda = .007022$.

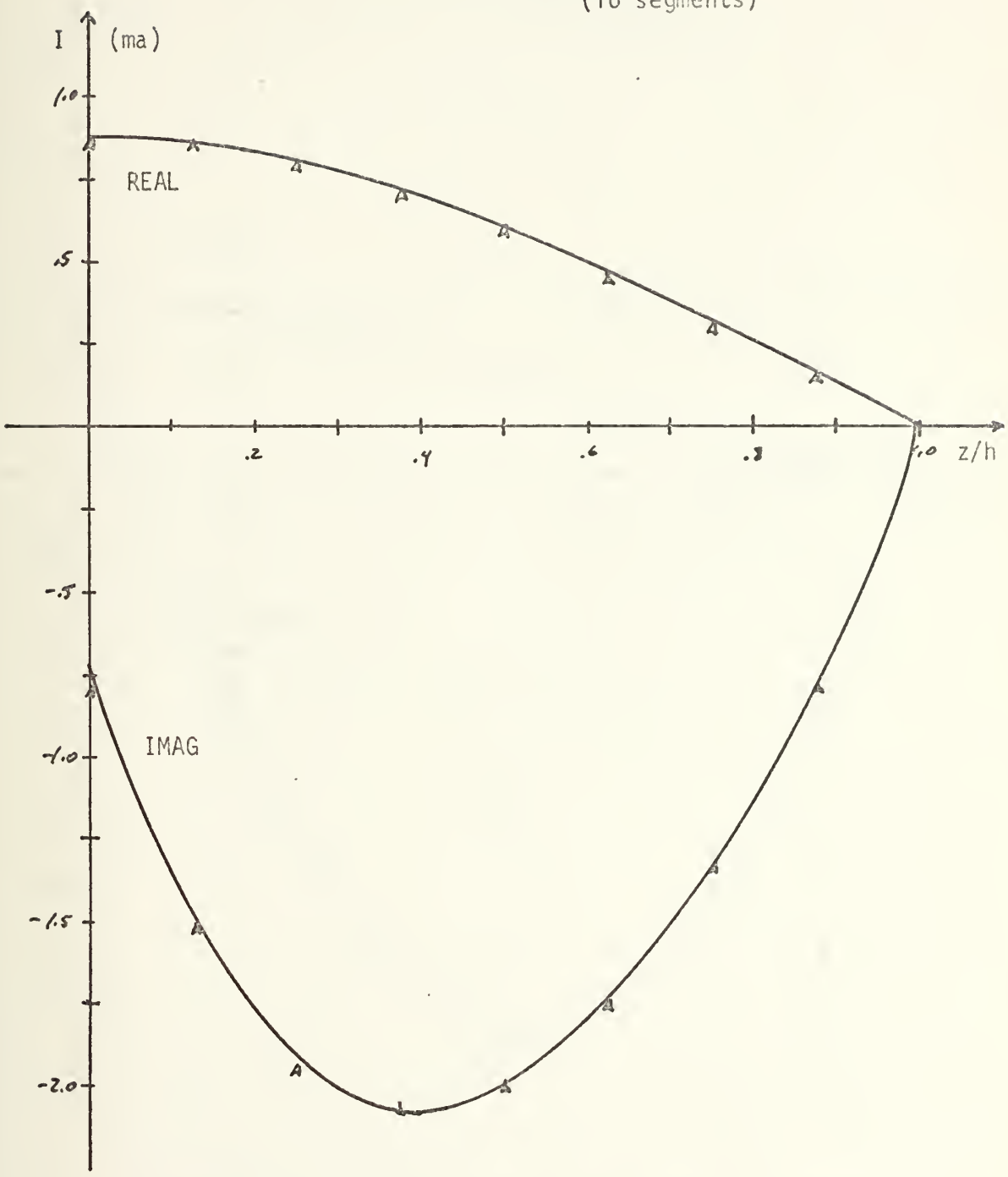

FIGURE 21. Current Distribution on a 3/4-wavelength dipole with radius $a/\lambda = .001588$.

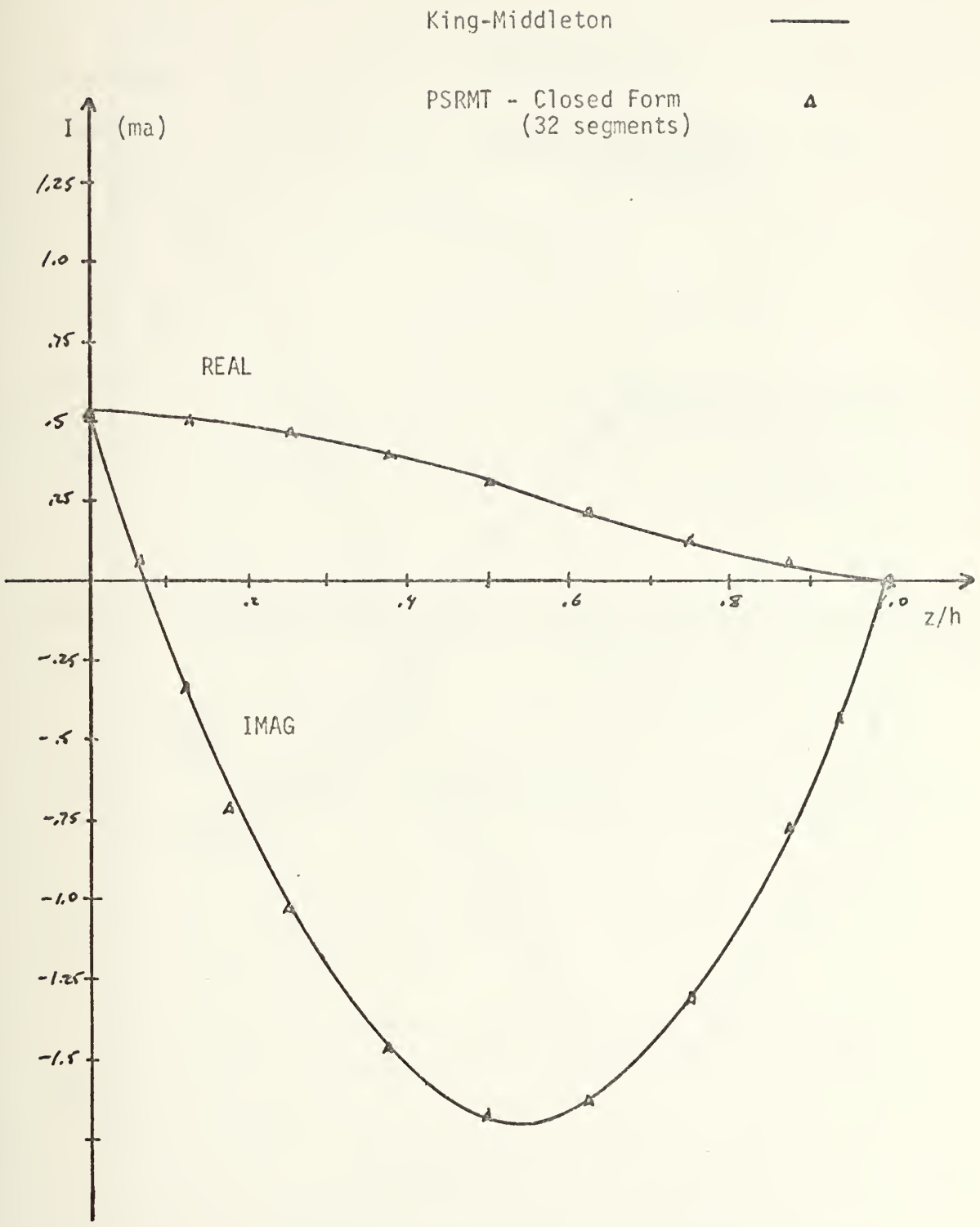

FIGURE 22. Current distribution on a full-wave dipole of radius $a/\lambda = .001588$.

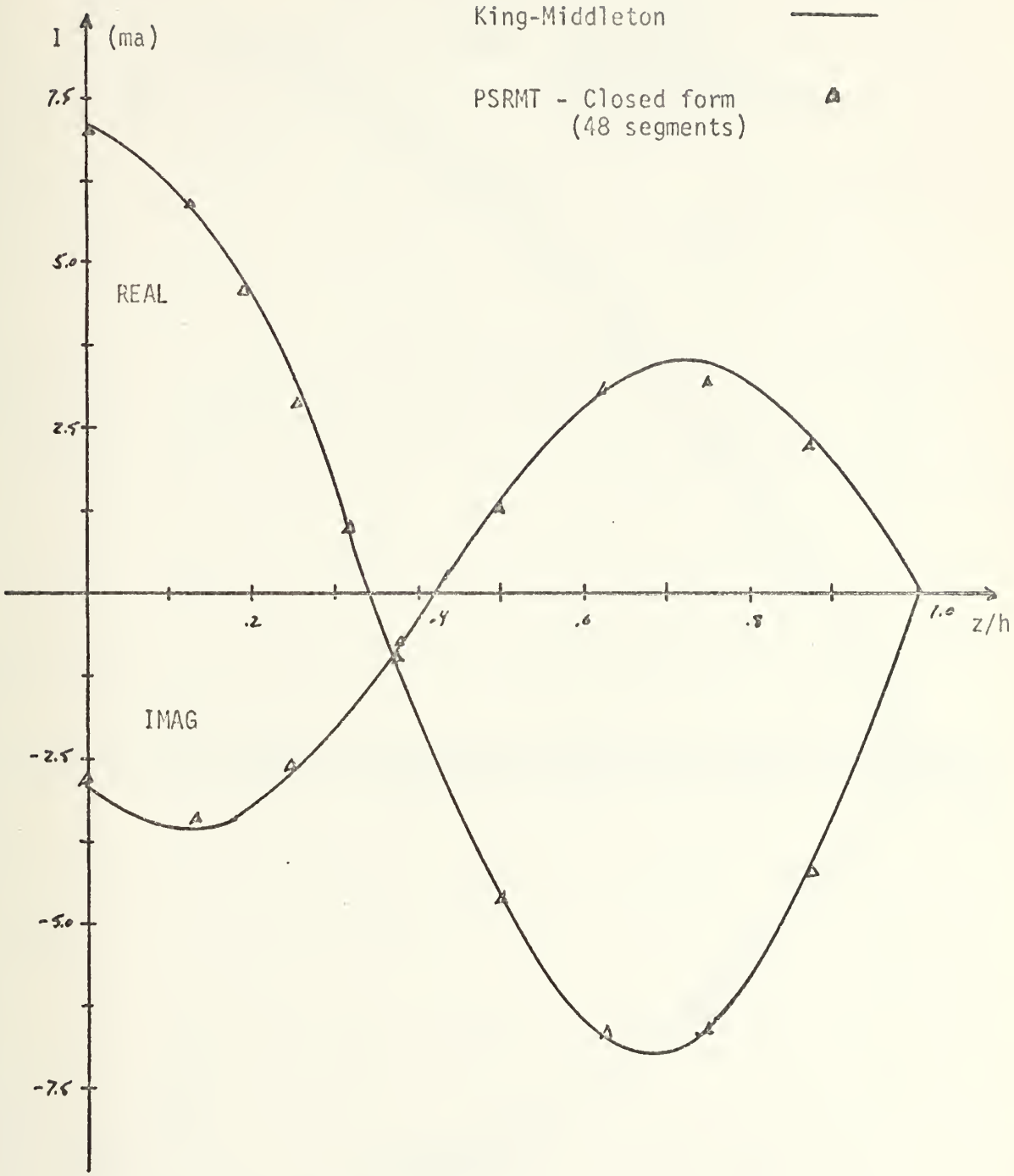

FIGURE 23. Current distribution on a 3/2 λ dipole of radius $a/\lambda = .001588$.

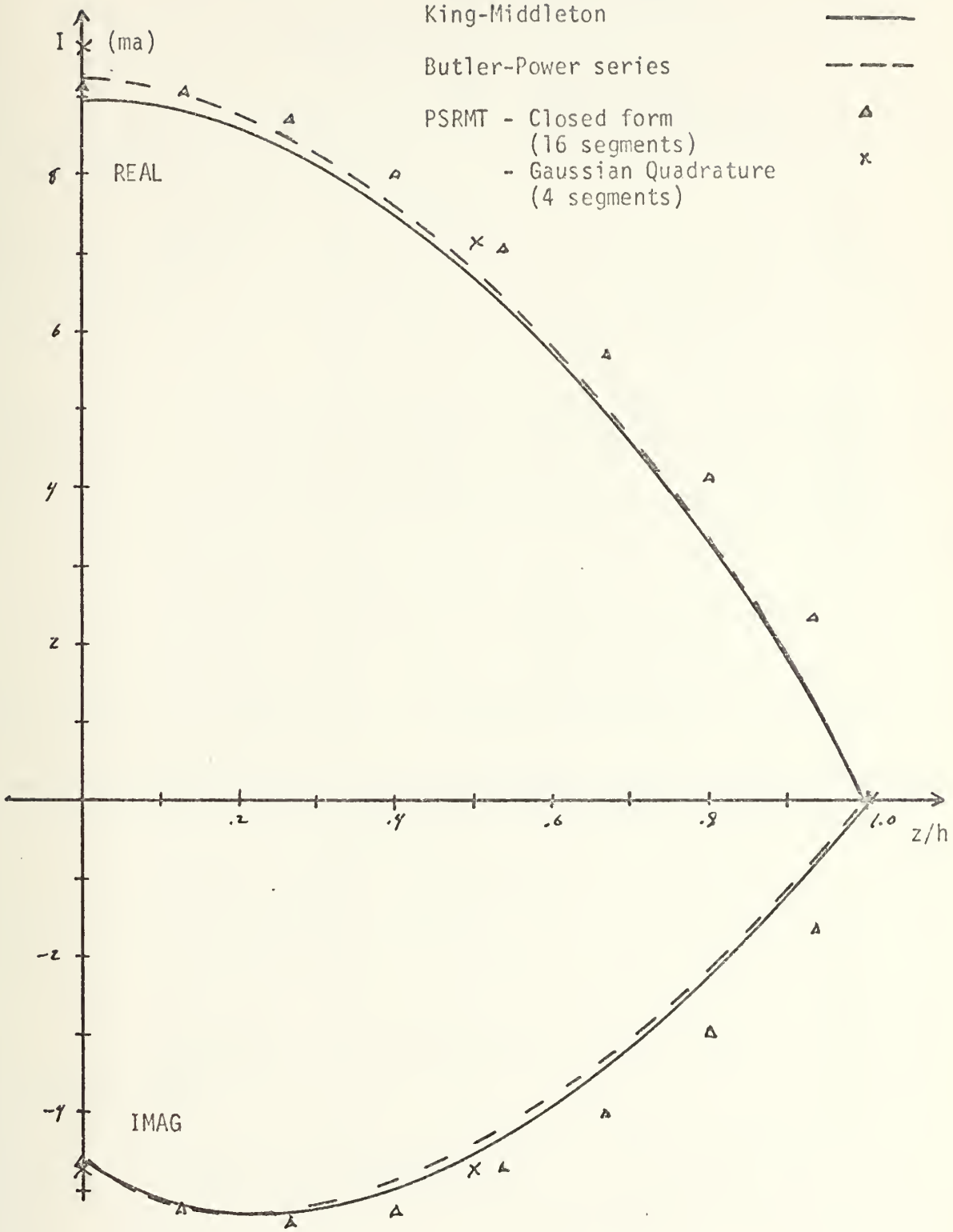

FIGURE 24. Current distribution on a half-wave dipole with radius $a/\lambda = .001588$.

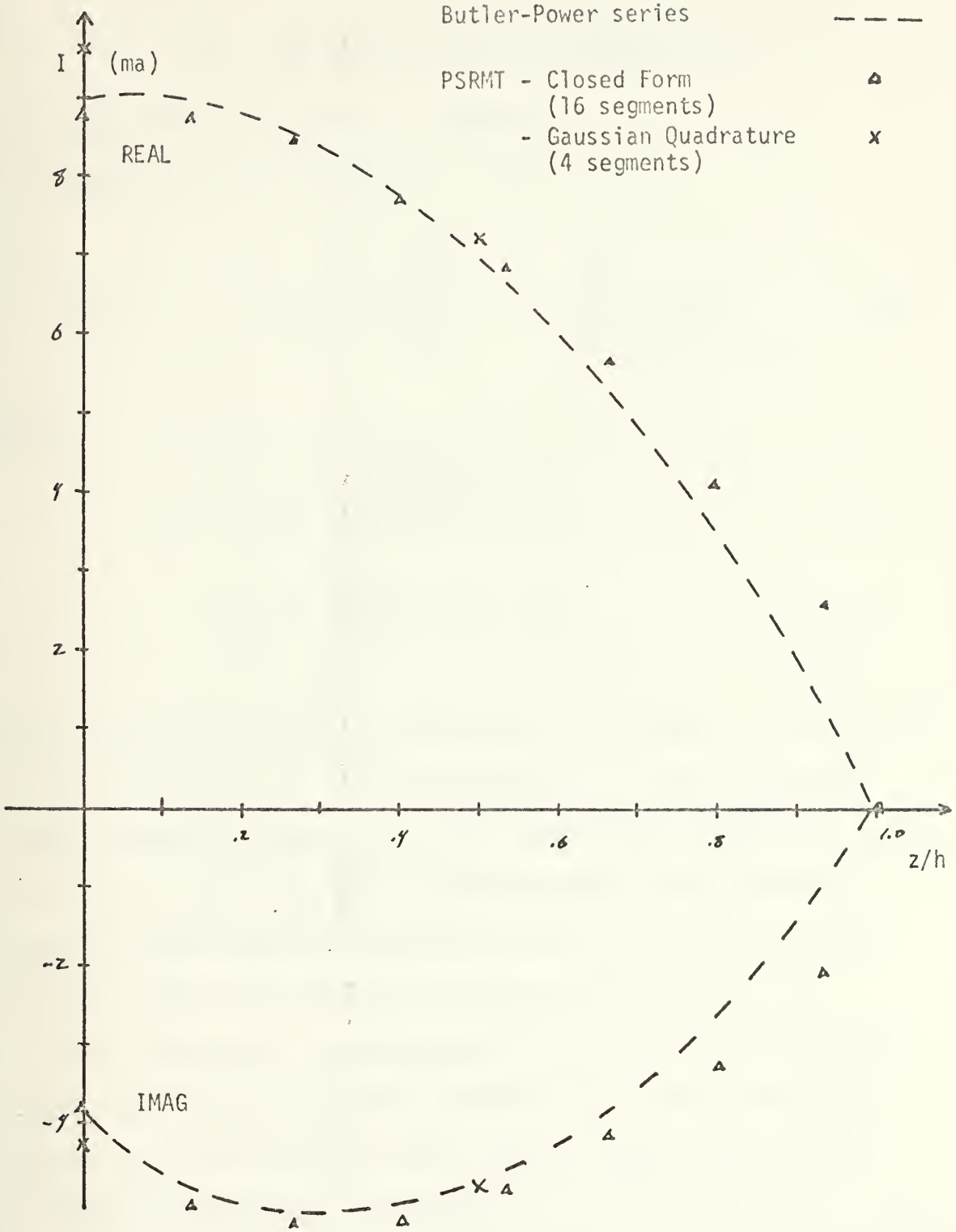

FIGURE 25. Current distribution on a half-wave dipole with radius $a/\lambda = .005$.

VII. CONCLUSIONS AND RECOMMENDATIONS

A. EVALUATION OF POTENTIAL INTEGRALS

Integrals of the form

$$F(z) = \int_0^h f(z') \left[\frac{e^{-jR_1}}{R_1} + \frac{e^{-jR_2}}{R_2}\right] dz' \qquad (50)$$

where

$$R_1 = \sqrt{(z-z')^2 + a^2}$$

$$R_2 = \sqrt{(z+z')^2 + a^2}$$

are extremely difficult to evaluate for "small a" because of the sharp peak in the integrand at $z' = z$. Although PSRMT has been formulated on the thin-wire assumption ($a << \lambda$); for very small radius values the integrand in Equation (34) becomes ill-behaved due to the form of the electric field $\bar{E}_m$ (refer to Equation (35)).

This phenomena was observed in the calculation of the input impedance of Figures 6 and 7. In fact, for $h/\lambda < .3$ the value of the radius ($h/a = 2000$) became small enough to thwart computation entirely.

B. APPLICATION OF THE GENERAL PSRMT TECHNIQUE

Although this paper dealt in particular with parallel dipoles only, PSRMT is useful in solving a wide variety of thin-wire antenna problems. With the aid of the concepts of reciprocity, reaction and surface equivalence, this technique reduces an integral equation to a set of simultaneous linear equations. This set of equations is readily solved on a computer to obtain the input impedance and current distribution on the antenna.

Richmond and Geary [16] presented a new form for the rigorous near-zone field of the linear dipole with sinusoidal current distribution. This electric field expression was employed to derive a closed form expression for the mutual impedance between coplanar-skew dipoles. By employing their expression for mutual impedance, complex geometries and surfaces may be represented by wire grids and reaction enforced to yield solutions.

C. RECOMMENDATIONS

The theory developed in this paper is by no means restrictive to the specific problem investigated. The data comparisons were made by employing PSRMT to equally segmented, thin-wire linear, parallel dipoles. Extensions to this problem are obvious. First, the segments need not be of equal length. By merely altering the computer program, the specific segment lengths can be applied to the appropriate formulas to generate a more general solution. Second,

the dipoles need not be parallel. By employing Richmond and Geary's closed form expression, the mutual impedance between any two coplanar elements may be determined. But now the reaction between the filamentary test dipole and the equivalent filamentary tubular surface dipole must be examined in more detail. In the case of parallel elements, the reaction applied between the test dipole and any filamentary surface dipole is the same. But due to the geometry of the problem involving two non-parallel segments, the mutual impedance depends upon the angular position of the filamentary surface dipole with respect to the axis. The question of how does one best react these segments is yet to be answered. E. G. Neely will present a Master's Degree Thesis to the Electrical Engineering Department at the U. S. Naval Postgraduate School (in September 1973), in which he deals with arbitrarily bent monopoles above a ground plane. He is approaching this problem by averaging the reactions taken around the circumference of the tubular dipole successively. Other approaches might be investigated.

APPENDIX A

TRANSFORMATION OF EXPONENTIAL INTEGRALS INTO CLOSED FORM EXPRESSIONS

The z component of the electric field from a dipole with a time-harmonic current distribution on each segment is expressed by Equation (35). For the mth test dipole, the dipole mode current distribution is shown in Figure 26.

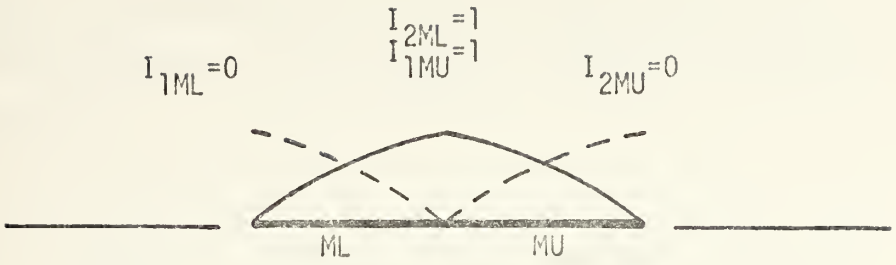

FIGURE 26. Typical mode current distribution for a filamentary test dipole.

From the expressions for the derivatives of the current at the endpoints of the segments (given in Equation (24)), one obtains

$$I'_{1ML} = k(I_{2ML} - I_{1ML} \cos kd) / \sin kd \qquad (51A)$$

$$I'_{2ML} = k(I_{2ML} \cos kd - I_{1ML}) / \sin kd \qquad (51B)$$

$$I'_{1MU} = k(I_{2MU} - I_{1MU} \cos kd) / \sin kd \qquad (51C)$$

$$I'_{2MU} = k(I_{2MU} \cos kd - I_{1MU}) / \sin kd \qquad (51D)$$

Note that from Figure 26, it is apparent that

$$I_{1ML} = 0 \qquad (52A)$$

$$I_{2ML} = I_{1MU} = 1 \qquad (52B)$$

$$I_{2MU} = 0 \qquad (52C)$$

The result of substituting Equation (52) into Equation (51) is

$$I'_{1ML} = -I'_{2MU} = k / \sin kd \qquad (53A)$$

$$I'_{2ML} = -I'_{1MU} = k \cos kd / \sin kd \qquad (53B)$$

Redefine the distance designations of Figure 5 according to Figure 27.

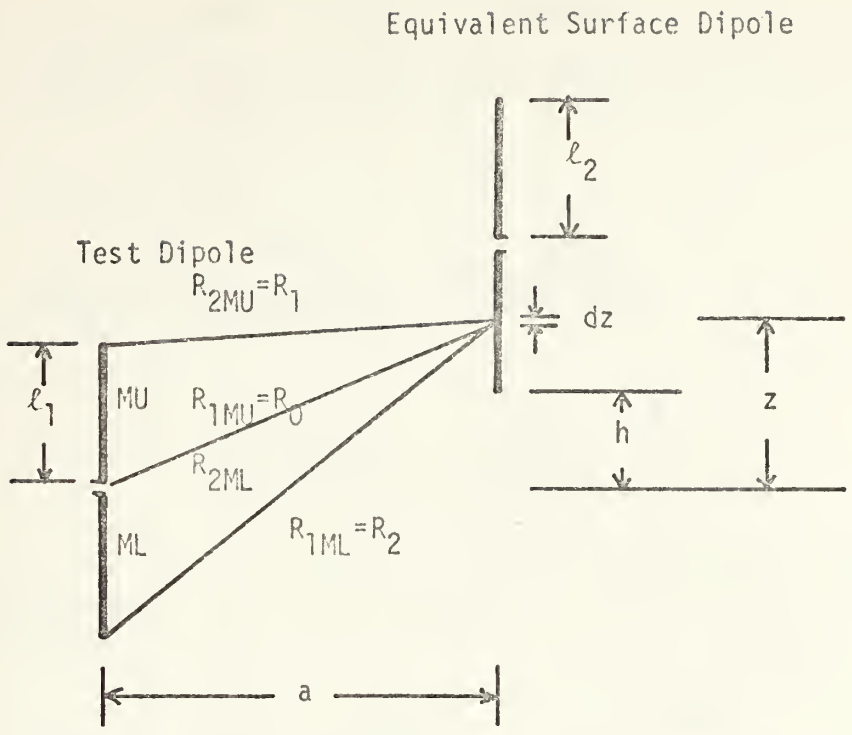

FIGURE 27. Geometry of two parallel dipoles in echelon.

With the geometry indicated in Figure 27 and Equation (53) the electric field of Equation (35) may be rewritten as

$$\bar{E}_m = \frac{\hat{z}}{4\pi j\omega\varepsilon}\left\{ \frac{k\, e^{-jkR_1}}{R_1 \sin kd} + \frac{k\, e^{-jkR_2}}{R_2 \sin kd} - 2k \cos kd \; \frac{e^{-jkR_0}}{R_0 \sin kd} \right\} \tag{54}$$

or equivalently:

$$\bar{E}_m = j\left(\frac{k}{4\pi\omega\varepsilon}\right) \hat{z}\left\{ - \frac{k\, e^{-jkR_1}}{R_1 \sin kd} - \frac{k\, e^{-jkR_2}}{R_2 \sin kd} + 2k \cos kd \; \frac{e^{-jkR_0}}{R_0 \sin kd} \right\} \tag{55}$$

In this problem

$$k = 2\pi / \lambda \qquad \text{with} \quad \lambda = v/f = 1$$

$$\omega = 2\pi(3(10^8))$$

$$\varepsilon = 1/36\pi\ (10^{-9})$$

therefore

$$k/4\pi\omega\varepsilon = 30 \ . \tag{56}$$

Equation (55) in light of Equation (56) is

$$\bar{E}_m = \frac{j\ 30\ \hat{z}}{\sin kd}\left\{\frac{e^{-jkR_1}}{R_1} - \frac{e^{-jkR_2}}{R_2} + 2\cos kd\ \frac{e^{-jkR_0}}{R_0}\right\} \tag{57}$$

where

$$R_0 = \sqrt{a^2 + z^2} \tag{58A}$$

$$R_1 = \sqrt{a^2 + (\ell_1 - z)^2} \tag{58B}$$

$$R_2 = \sqrt{a^2 + (\ell_1 + z)^2} \tag{58C}$$

Employing the trigonometric identity

$$\sin 2\alpha = 2 \sin\alpha \cos\alpha \ ,$$

Equation (57) may be written as

$$\bar{E}_m = \frac{30\ \hat{z}}{\sin kd}\left\{\frac{-j\ e^{-jkR_1}}{R_1} + \frac{-j\ e^{-jkR_2}}{R_2} + \frac{2j\ \cos kd\ e^{-jkR_0}}{R_0}\right\} . \tag{59}$$

Equation (59) is exactly the form that H. E. King expressed his electric field in; except for the extra "sin kd" term in the denominator. This term is not present in King's expression for the electric field because he was assuming

that the antenna current distribution is sinusoidal. In the application of PSRMT the current distributions are assumed to be piecewise-sinusoidal and therefore the expression for the mutual impedance is:

$$Z_{mn} = \frac{-30}{(\sin kd)^2}\left[\left\{\int_{\ell_{n-1}}^{\ell_n} \sin k\,(\ell - \ell_{n-1}) + \int_{\ell_n}^{\ell_{n+1}} \sin k(\ell_{n+1} - \ell)\right\}\left(\frac{-j\,e^{-jkR_1}}{R_1} + \frac{-j\,e^{-jkR_2}}{R_2} + \frac{2j\cos kd\,e^{-jkR_0}}{R_0}\right) d\ell\right] \tag{60}$$

Equation (60) follows from the substitution of Equation (59) into Equation (34) and assuming that the length of all segments are equal to d.

In order to facilitate transforming Equation (60) into a closed form expression, Z_{mn} will be expressed in terms of the geometry of Figure 27. For sinusoidal current distributions,

$$Z_{mn} = -30\left[\left\{\int_{h}^{\ell_2+h} \sin k(z - h) + \int_{\ell_2+h}^{2\ell_2+h} \sin k(2\ell_2+h-z)\right\}\left(\frac{-j\,e^{-jkR_1}}{R_1} + \frac{-j\,e^{-jkR_1}}{R_2} + \frac{2j\cos k_1 d\,e^{-jkR_0}}{R_0}\right) dz\right] \tag{61}$$

Obviously Equation (61) can be multiplied out to yield six expressions, one of which follows:

$$a = +30 \int_{\ell_2+h}^{2\ell_2+h} \sin k(2\ell_2 + h - z) \left(\frac{+j\, e^{-jkR_1}}{R_1} \right) dz. \tag{62}$$

Employing the trigonometric relations:

$$e^{j\alpha} = \cos \alpha + j \sin \alpha \tag{63A}$$

$$\sin \alpha = -\sin (-\alpha) \tag{63B}$$

$$\cos \alpha = \cos (-\alpha) \quad , \tag{63C}$$

Equation (62) becomes

$$a = 30 \int_{\ell_2+h}^{2\ell_2+h} \left(\frac{j \cos kR_1}{R_1} + \frac{\sin kR_1}{R_1} \right) \sin k(2\ell_2+h-z)dz \tag{64}$$

The real part of complex Equation (61) gives the mutual resistance and the imaginary part gives the mutual reactance. The real part of Equation (64) gives only one-sixth of the total expression for the mutual resistance, but it will now be transformed into a closed form expression in order to illustrate the procedure of obtaining all twelve terms, both resistive and reactive.

$$A_{REAL} = 30 \int_{\ell_2+h}^{2\ell_2+h} \left(\frac{\sin kR_1}{R_1}\right) \sin k(2\ell_2 + h - z)\, dz \tag{65}$$

Substitute the expression for R_1 given in Equation (58) to obtain

$$A_{REAL} = 30 \int_{\ell_2+h}^{2\ell_2+h} \frac{\sin k\sqrt{a^2 + (\ell_1 - z)^2}}{\sqrt{a^2 + (\ell_1 - z)^2}} \sin k(2\ell_2+h-z)\, dz. \tag{66}$$

By a change in the variable of $x = \ell_1 - z$, Equation (66) becomes

$$A_{REAL} = -30 \int_{\ell_1-\ell_2-h}^{\ell_1-2\ell_2-h} \left(\frac{\sin k\sqrt{A^2 + x^2}}{\sqrt{A^2 + x^2}}\right) \sin k(2\ell_2+h-\ell_1+x)\, dx. \tag{67}$$

Employing the trigonometric identity for the product of angles one obtains

$$A_{REAL} = +15 \int_{\ell_1-\ell_2-h}^{\ell_1-2\ell_2-h} [-\cos k(h-\ell_1+2\ell_2) \cos k(\sqrt{a^2+x^2} - x$$

$$- \sin k(h - \ell_1 + 2\ell_2) \sin k(\sqrt{a^2+x^2} - x)$$

$$+ \cos k(h - \ell_1 + 2\ell_2) \cos k(\sqrt{a^2+x^2} + x)$$

$$- \sin k(h - \ell_1 + 2\ell_2) \sin k(\sqrt{a^2+x^2} + x)] \cdot \frac{dx}{\sqrt{a^2+x^2}} \quad . \tag{68}$$

A second change of variable of

$$u = k(\sqrt{a^2+x^2} - x) \tag{69A}$$

$$v = k(\sqrt{a^2+x^2} + x) \tag{69B}$$

gives

$$A_{REAL} = 15 \int_{u_1}^{u_3} [+\cos k(h - \ell_1 + 2\ell_2) \frac{\cos u}{u} \, du$$

$$+\sin k(h - \ell_1 + 2\ell_2) \frac{\sin u}{u}] \, du$$

$$+ 15 \int_{v_1}^{v_3} [+\cos k(h - \ell_1 + 2\ell_2) \frac{\cos v}{v} \, dv$$

$$-\sin k(h - \ell_1 + 2\ell_2) \frac{\sin v}{v}] \, dv \tag{70}$$

where

$$u_1 = k(\sqrt{a^2 + (h - \ell_1 + \ell_2)^2} + (h - \ell_1 + \ell_2))$$

$$u_3 = k(\sqrt{a^2 + (h - \ell_1 + 2\ell_2)^2} + (h - \ell_1 + 2\ell_2))$$

$$v_1 = k(\sqrt{a^2 + (h - \ell_1 + \ell_2)^2} - (h - \ell_1 + \ell_2))$$

$$v_3 = k(\sqrt{a^2 + (h - \ell_1 + 2\ell_2)^2} - (h - \ell_1 + 2\ell_2)) \quad .$$

The integrals of Equation (70) are recognized as sine and cosine integrals and may be written as

$$A_{REAL} = 15 \Big(\cos k(\ell_1 - 2\ell_2 - h) \, [-Ci(u_1) - Ci(v_1) + Ci(u_3) + Ci(v_3)]$$

$$+ \sin k(\ell_1 - 2\ell_2 - h) \, [Si(u_1) - Si(v_1) - Si(u_3) + Si(v_3)] \Big) \qquad (71)$$

Recall that Equation (61) through Equation (70) was written for sinusoidal current distributions. To make them applicable to piecewise-sinusoidal current distributions, Equation (61) must be multiplied by the factor $1/(\sin kd)^2$.

Equation (61) expanded in closed form as typified by Equation (71) is written in its entirety in Equation (72) and (73) in Appendix B. Equation (73) is an expression for the mutual impedance between two thin parallel center-fed

antennas with half-lengths HL spaced a distance DL apart and staggered by the value SL. This expression is a simplification of H. E. King's general formula for mutual impedance [10].

APPENDIX B

FORTRAN PROGRAM LISTING

Figure 28 is the main computer program listing (in Fortran IV) for the solution of the linear dipole antenna's driving point admittance and current distribution.

The symbols for the input data are defined as:

EL length of the dipole in wavelengths

A radius of the dipole

N number of antenna segments.

This program has built in "do-loop" that generates the voltage matrix of Equation (41). The voltage source of one volt is automatically placed at the center junction of the dipole.

Calculation of the complex Z_{mn} matrix is done in the subroutine CZMN2. This calculation may be performed by one of several techniques. Gaussian Quadrature, Romberg and Weddle's methods can be employed in order to effect numerical integration of Equation (34) for Z_{mn}. If this is done, additional subroutines are required to calculate the electric field explicitly, establish the limits of integration, perform the necessary integration technique,

etc.. Z_{mn} may be most efficiently calculated by programming directly the closed form expression of Equation (73).

Once Z_{mn} was determined, CMIN1, a subroutine developed by E. G. Neely, was used to calculate the complex inverse of Z_{mn}. The complex current coefficients result from a direct application of Equation (40). Since a single one volt source was placed at the center junction, the driving point admittance is known immediately from Equation (43).

The program's output is set up to provide a.) an echo check on the input parameters and important variables, b.) list the real and imaginary parts of the complex junction currents as a function of z/h, c.) list the magnitude and phase of junction currents, and d.) display the input admittance and impedance. This output is presented for both the dipole and the monopole.

FORTRAN LISTING OF MAIN PROGRAM AND SUBROUTINE CZMN|

AN APPLICATION OF PSRMT TO LINEAR, PARALLEL DIPOLE ANTENNAS

BY MICHAEL L. BRYANT
UNDER THE DIRECTION OF DR. RICHARD W. ADLER

JAN-JUN/73

```
//  EXEC  FORTCLG,REGION.GO=100K
//FORT.SYSIN  DD  *
      IMPLICIT REAL*4(L),COMPLEX*8(C)
      REAL*4 TWOPI/6.283185/
C
C
      DIMENSION VOLT(64),CZMN(64,64),CURR(64)
      DIMENSION AMAG(64),APHASE(64),APHDEG(64)
      DIMENSION CURRMP(64),AMAGMP(64),ZOH(64)
C
CC
CC          SPECIFICATION OF MEMORY STORAGE LOCATIONS
C
      COMMON/INPUTS/A,EL,N,FREQ,NX
      COMMON/COMPUT/ACONST,BETA,D
C
CC
CC          INPUT PARAMETERS TO BE MODIFIED ON SUBSEQUENT RUNS
C
      A=0.001588
      EL=0.5
      DO 995 N=24,36,6
      FREQ=3.0E8
C
CC
CC          CALCULATION OF CONSTANTS
C
      OMEGA=TWOPI*FREQ
      WAVE=3.0E8/FREQ
      BETA=TWOPI/WAVE
      D=EL/FLOAT(N)
      H=EL/2.0
```

```
      NLESS1=N-1
      NSUB=N/2
      NSUBM1=NSUB-1
      BETAH=BETA*(EL/2.0)
      HWAVE=(EL/2.0)/WAVE
      BETAA=BETA*A
      AWAVE=A/WAVE
C
CC
CC          GENERATE DESIRED VOLTAGE MATRIX
C
      DO 2 J=1,NLESS1
      VOLT(J)=0.0
    2 CONTINUE
      VOLT(NSUB)=(1.0)
C
CC
CC          ECHO CHECK ON DATA AND COMPUTED CONSTANTS
C
      WRITE(6,4)
    4 FORMAT('1',5X,'INPUT PARAMETERS TO BE MODIFIED ON SUBSEQUENT RUNS'
     *      ////)
      WRITE(6,5) EL
    5 FORMAT('0',T20,'ANTENNA LENGTH (L)',T60,F8.4//)
      WRITE(6,6) H
    6 FORMAT('0',T20,'ANTENNA HALFLENGTH (H)',T60,F8.4//)
      WRITE(6,7) N
    7 FORMAT('0',T20,'NUMBER OF ANTENNA SEGMENTS (N)',
     *      T60,I3//)
      WRITE(6,8) D
    8 FORMAT('0',T20,'LENGTH OF SEGMENTS (D)',T60,F10.6//)
      WRITE(6,11) NX
   11 FORMAT('0',T20,'NUMBER OF INTEGRATION POINTS (NX)',T60,I3///////)
      WRITE(6,9) FREQ
    9 FORMAT('0',T20,'FREQUENCY (F)',T40,1PE11.3//)
      WRITE(6,10) OMEGA
   10 FORMAT('0',T20,'FREQUENCY (W)',T40,1PE11.3///////)
   12 FORMAT('0',T40,'WAVELENGTH (LAMBDA)',T70,F11.7//)
      WRITE(6,12) WAVE
      WRITE(6,13) BETA
   13 FORMAT('0',T40,'BETA (K0)' ,T70,F11.7///////)
      WRITE(6,15) BETAH
   15 FORMAT('0',T20,'K0H',T60,F11.7//)
      WRITE(6,16) HWAVE
   16 FORMAT('0',T20,'H/LAMBDA',T60,F11.7//)
      WRITE(6,17) BETAA
   17 FORMAT('0',T20,'K0A',T60,F11.7//)
      WRITE(6,18) AWAVE
```

```
   18 FORMAT('0',T20,'A/LAMBDA',T60,F11.7//)
      WRITE(6,111)
C
CCC
CCC         CALCULATION OF COMPLEX ZMN MATRIX
CCC
      DO 200 M=1,NLESS1
      DO 100 NM1=1,NLESS1
C
      CZMN(M,NM1)=CZMN2(M,NM1)
C
C
  100 CONTINUE
  200 CONTINUE
CCCC
CCCC        CALCULATION OF COMPLEX ZMN MATRIX INVERSE
CCCC
      CALL CMIN1(NLESS1,CZMN,NDIM,DETERM)
CCCCC
CCCCC
CCCCC       CALCULATION OF COMPLEX CURRENT MATRIX
CCCCC
      DO 135 M=1,NLESS1
      CURR(M)=(0.0,0.0)
      DO 136 NM1=1,NLESS1
      CURR(M)= CURR(M)+CZMN(M,NM1)*VOLT(NM1)
  136 CONTINUE
      CURR(M)=CURR(M)*1000.0
      CURRMP(M)=CURR(M)*2.0
      ZOH(M)=FLOAT(M-NSUB)*(2.0/FLOAT(N))
  135 CONTINUE
      WRITE(6,149)
  149 FORMAT(10X,'COMPLEX JUNCTION CURRENTS (MILLIAMPS)'///)
      WRITE(6,150)
  150 FORMAT('0',20X,'Z/H',30X,'MONOPOLE',35X,'DIPOLE'//)
      WRITE(6,151)(ZOH(J),CURR(J),J=1,NSUBM1)
  151 FORMAT('0',13X,F10.4,T80,2F15.4)
      WRITE(6,152)(ZOH(J),CURRMP(J),CURR(J),J=NSUB,NLESS1)
  152 FORMAT('0',13X,F10.4,T41,2F15.4,T80,2F15.4)
      WRITE(6,111)
  111 FORMAT('0'/////)
C
CCC
CCC         CALCULATION OF CURRENT MAGNITUDE AND PHASE
C
      DO 155 J=1,NLESS1
      AMAG(J)=CABS(CURR(J))
```

```
      AMAGMP(J)=AMAG(J)*2.0
      APHASE(J)=ATAN2(AIMAG(CURR(J)),REAL(CURR(J)))
      APHDEG(J)=APHASE(J)*57.29578
  155 CONTINUE
      WRITE(6,156)
  156 FORMAT(10X,'COMPLEX JUNCTION CURRENTS - MAGNITUDE (MILLIAMPS)',
     *   20X,'PHASE (RADIANS)',15X,'PHASE (DEGREES)'///)
      WRITE(6,157)
  157 FORMAT(10X,'Z/H',14X,'MONOPOLE',15X,'DIPOLE'//)
      WRITE(6,158)(ZOH(J),AMAG(J),APHASE(J),APHDEG(J),J=1,NSUBM1)
  158 FORMAT('0',2X,F10.4,T43,F15.4,T79,F10.3,21X,F10.3)
      WRITE(6,159)(ZOH(J),AMAGMP(J),AMAG(J),APHASE(J),APHDEG(J),
     *   J=NSUB,NLESS1)
  159 FORMAT('0', 2X,F10.4,T20,F15.4,T43,F15.4,T79,F10.3,21X,F10.3)
      WRITE(6,111)
C
CCC
CCC        CALCULATION OF COMPLEX INPUT ADMITTANCE (MILLIMHOS)
C
      CADM=CURR(NSUB)
      CADMMP=CADM*2.0
      WRITE(6,160) CADMMP
  160 FORMAT('0',9X,'COMPLEX INPUT ADMITTANCE (MILLIMHOS)',T60,
     *   'MONOPOLE',T70,2F15.4///)
      WRITE(6,161) CADM
  161 FORMAT('0',T60,'DIPOLE',T70,2F15.4//////)
C
CCC
CCC        CALCULATION OF COMPLEX INPUT IMPEDENCE (OHMS)
C
      CIMP=1.0E3/CADM
      CIMPMP=CIMP*0.5
      WRITE(6,170) CIMPMP
  170 FORMAT('0',9X,'COMPLEX INPUT IMPEDENCE (OHMS)',T60,
     *   'MONOPOLE',T70,2F15.4///)
      WRITE(6,171) CIMP
  171 FORMAT('0',T60,'DIPOLE',T70,2F15.4//////)
C
  995 CONTINUE
C
      END
```

```
      COMPLEX FUNCTION CZMN1(DL,HL,SL)
C
C
C     THE SUBROUTINE CZMN1 COMPUTS THE COMPLEX MUTUAL IMPEDENCE
C     BETWEEN TWO LINEAR, PARALLEL DIPOLE ANTENNAS
C
C
C     DESCRIPTION OF ARGUMENTS
C
C           DL  -  DISTANCE BETWEEN DIPOLES
C           HL  -  LENGTH OF DIPOLE ARM IN WAVELENGTHS (H/LAMBDA)
C           SL  -  STAGGER OF DIPOLES (REFER TO FIGURE 27)
C
C
C     REMARKS
C
C           MUTUAL IMPEDENCE TERM FORMULATED BY F. E. KING
C           FORM ADAPTED BY J. H. RICHMOND
C
C
C           SUBROUTINE SICI (STANDARD IBM/360 ROUTINE) IS USED TO
C           EVALUATE THE SINE AND COSINE INTEGRALS.
C
      REAL L,LE,LL
      B=6.2831853
C
C     ESTABLISH BASIC CONSTANTS FROM ARGUMENTS
C
      D=DL
      L=HL
      LE=HL
      HC=SL
      BLE=B*LE
      H=ABS(HC)-L
      LL=LE
      HPL=H+LL
      HP2L=H+2.0*LL
      HP3L=H+3.0*LL
      HML=H-LL
C
C           COMPUTATION OF REPEATED FACTORS
C
      SBL=SIN(BLE)
```

```
      CBL=COS(BLE)
      SBH=SIN(B*H)
      CBH=COS(B*H)
      SBHML=SIN(B*HML)
      CBHML=COS(B*HML)
      SBHPL=SIN(B*HPL)
      CBHPL=COS(B*HPL)
      SBHP2L=SIN(B*HP2L)
      CBHP2L=COS(B*HP2L)
      SBHP3L=SIN(B*HP3L)
      CBHP3L=COS(B*HP3L)
C
C
C           DEFINE ARGUMENTS FOR THE SICI SUBRCUTINE
C
      TEMP=SQRT(D*D+H*H)+H
      V1=B*D*D/TEMP
      U1=B*TEMP
      TEMP=SQRT(D*D+HML*HML)+HML
      UC=B*TEMP
      V0=B*D*D/TEMP
      TEMP=SQRT(D*D+HPL*HPL)+HPL
      U3=B*TEMP
      V3=B*D*D/TEMP
      TEMP=SQRT(D*D+HP2L*HP2L)+HP2L
      U2=B*D*D/TEMP
      V2=B*TEMP
      TEMP=SQRT(D*D+HP3L*HP3L)+HP3L
      U4=B*D*D/TEMP
      V4=B*TEMP
C
      CALL SICI (SIU0,CIU0,U0)
      CALL SICI (SIU1,CIU1,U1)
      CALL SICI (SIV2,CIV2,V2)
      CALL SICI (SIV4,CIV4,V4)
      CALL SICI (SIU3,CIU3,U3)
      CALL SICI (SIV1,CIV1,V1)
      CALL SICI (SIV0,CIV0,V0)
      CALL SICI (SIV3,CIV3,V3)
      CALL SICI (SIU2,CIU2,U2)
      CALL SICI (SIU4,CIU4,U4)
```

```
C  CALCULATION OF THE RESISTIVE COMPONENT OF THE MUTUAL IMPEDENCE

      R=15.0*(CBHML*(CIU0+CIV0-CIU1-CIV1)-SBHML*(-SIU0+SIV0+SIU1-SIV1)+C    (72A)
     2BHPL*(2.*CIV3+2.*CIU3-CIU2-CIV2-CIU1-CIV1)+SBHPL*(-SIV3+SIU3+SIU2-
     3SIV2-SIU1+SIV1+SIU3-SIV3)+CBHP3L*(-CIU2-CIV2+CIU4+CIV4)+SBHP3L*(SI
     4U2-SIV2-SIU4+SIV4) +2.*CBL*CBH*(-CIV1-CIU1+CIV3+CIU3)+2.*CBL*SBH*(
     5SIV1-SIU1-SIV3+SIU3)+2.*CBL*CBHP2L*(CIV3+CIU3-CIU2-CIV2)+2.*CBL*SB
     6HP2L*(-SIV3+SIU3+SIU2-SIV2))

C  CALCULATION OF THE REACTIVE COMPONENT OF THE MUTUAL IMPEDENCE

      X=15.0*(CBHML*(-SIU0-SIV0+SIU1+SIV1)-SBHML*(-CIU0+CIV0+CIU1-CIV1)+    (72B)
     2CBHPL*(-2.*SIV3-2.*SIU3+SIU2+SIV2+SIU1+SIV1)+SBHPL*(-2.*CIV3+2.*C
     3IU3+CIU2-CIV2-CIU1+CIV1)+CBHP3L*(SIU2+SIV2-SIU4-SIV4)+SBHP3L*(CIU2
     4-CIV2-CIU4+CIV4)+2.*CBL*CBH*(SIV1+SIU1-SIV3-SIU3)+2.*CBL*SBH*(CIV
     51-CIU1-CIV3+CIU3)+2.*CBL*CBHP2L*(-SIV3-SIU3+SIU2+SIV2)+2.*CBL*SBHP
     62L*(-CIV3+CIU3+CIU2-CIV2))

C  FORMULATE ZMN FOR AN ASSUMED PIECEWISE-SINUSOIDAL CURRENT DISTRIBUTION

      CZMN1=CMPLX(R,X)/(SBL*SBL)                                            (73)

      RETURN
      END
```

BIBLIOGRAPHY

1. Brown, G. H., "Directional Antennas," Proceedings of IRE, Vol. 25, pp. 81-145, January 1937.

2. Butler, C. M., "Integral Equation Solution Methods," Supplementary Notes for Wire Antennas and Scatterers, A Short Course in Electromagnetic Theory presented at the University of Mississippi, April 1972.

3. Butler, C. M., "Outline of the Moment Method," Supplementary Notes for Wire Antennas and Scatterers, A Short Course in Electromagnetic Theory presented at the University of Mississippi, April 1972.

4. Carson, J., "A Generalization of the Reciprocal Theory," Bell System Technical Journal, Vol. 3, pp. 393-399, July 1924.

5. Carter, P. S., "Circuit Relations in Radiating Systems and Application to Antenna Problems," Proceedings of IRE, Vol. 20, pp. 1004-1041, June 1932.

6. Cox, C. R., "Mutual Impedance Between Vertical Antennas of Unequal Heights," Proceedings of IRE, Vol. 35, pp. 1367-1370, November 1947.

7. Crout, P. D., "A Short Method of Evaluating Determinants and Solving Systems of Linear Equations with Real or Complex Coefficients," AIEE Transactions (supplement), Vol. 60, pp. 1235-1241, December 1941.

8. Harrington, R. F., "Matrix Methods for Field Problems," Proceedings of the IEEE, Vol. 55, pp. 136-149, February 1967.

9. Harrington, R. F., Time-Harmonic Electromagnetic Fields, pp. 340-345, McGraw-Hill, 1961.

10. King, H. E., "Mutual Impedance of Unequal Length Antennas in Echelon," IRE Transactions on Antennas and Propagation, Vol. AP-5, pp. 306-313, July 1957.

11. King, R. W. P., Tables of Antenna Characteristics, pp. 27-49, IFI/Plenum, 1971.

12. Lewin, L., "Mutual Impedance of Wire Aerials," Wireless Engineer, Vol. 28, pp. 352-355, December 1951.

13. Richards, G. A., A Reaction Formulation and Numerical Results for Multiturn Loop Antennas and Arrays, Ph.D. Dissertation, The Ohio State University, June 1970.

14. Richmond, J. H., Coupled Linear Antennas with Skew Orientation, Report 2708-3, Electroscience Laboratory, prepared under Contract DAAD05-69-C-0031 for the Department of the Army, Aberdeen Proving Grounds, Maryland, August 1969.

15. Richmond, J. H., Computer Analysis of Three-Dimensional Wire Antennas, Report 2708-4, Electroscience Laboratory, prepared under Contract DAAD05-69-C-0031 for the Department of the Army, Aberdeen Proving Grounds, Maryland, August 1969.

16. Richmond, J. H., and Geary, N. H., "Mutual Impedance Between Coplanar-Skew Dipoles," IEEE Transactions on Antennas and Propagation, Vol. AP-18, pp. 694-696, September 1970.

17. Rumsey, V. H., "The Reaction Concept in Electromagnetic Theory," Physical Review, Ser. 2, Vol. 94, pp. 1483-1491, June 1954.

18. Schelkunoff, S. A., "On Diffraction and Radiation of Electromagnetic Waves," The Physical Review, Vol. 56, pp. 308-316, August 1939.

19. Schelkunoff, S. A., and Friis, H. T., Antennas: Theory and Practice, p. 401, Wiley, 1952.

20. Travieso-Diaz, M. F., Wire-Grid Reaction Solution of Electromagnetic Scattering and Radiation Problems, Report 2622-5, Harry Diamond Laboratories, prepared under Contract DAAG39-69-C-0061 for the Department of the Army, Washington, D. C., May 1971.

21. Tsai, L. L., "Richmond's Piecewise-Sinusoidal Reaction Technique," Supplementary Notes for Wire Antennas and Scatterers, A Short Course in Electromagnetic Theory Presented at the University of Mississippi, April 1972.

INITIAL DISTRIBUTION LIST

		No. Copies
1.	Defense Documentation Center Cameron Station Alexandria, Virginia 22314	2
2.	Library, Code 0212 Naval Postgraduate School Monterey, California 93940	2
3.	Asst. Professor Richard W. Adler, Code 52 Ab Department of Electrical Engineering Naval Postgraduate School Monterey, California 93940	1
4.	ENS Michael Lynn Bryant, USN 1115 East 20th Street Hutchinson, Kansas 67501	2
5.	Dr. Sydney R. Parker, Code 52 Department Chairman Department of Electrical Engineering Naval Postgraduate School Monterey, CA 93940	1

Security Classification

DOCUMENT CONTROL DATA - R & D

(Security classification of title, body of abstract and indexing annotation must be entered when the overall report is classified)

INATING ACTIVITY (Corporate author)

Naval Postgraduate School
Monterey, California 93940

2a. REPORT SECURITY CLASSIFICATION

Unclassified

2b. GROUP

ORT TITLE

An Application of the Piecewise-Sinusoidal Reaction Matching Technique to Linear Dipole Antennas

CRIPTIVE NOTES (Type of report and inclusive dates)

Master's Thesis; June 1973

HOR(S) (First name, middle initial, last name)

Michael Lynn Bryant

ORT DATE	7a. TOTAL NO. OF PAGES	7b. NO. OF REFS
June 1973	105	21

TRACT OR GRANT NO.	9a. ORIGINATOR'S REPORT NUMBER(S)
OJECT NO.	
	9b. OTHER REPORT NO(S) (Any other numbers that may be assigned this report)

TRIBUTION STATEMENT

Approved for public release; distribution unlimited.

PLEMENTARY NOTES	12. SPONSORING MILITARY ACTIVITY
	Naval Postgraduate School Monterey, California 93940

TRACT

This paper is an application of the Piecewise-Sinusoidal Reaction Matching Technique (PSRMT) to linear, parallel thin-wire dipoles. The "method of moments" is briefly outlined and the fundamental electromagnetic principles of reciprocity, surface equivalence and reaction are discussed. Through a logical combination of these concepts, PSRMT is developed and applied to thin-wire dipoles radiating in free space due to a delta function voltage generator at their center. The driving point impedance and the current distribution are calculated and compared to results obtained from other independent theoretical techniques.

The major contribution of this investigation is not that of presenting a new technique for calculating the input impedance and current distributions on dipole antennas. The study is primarily concerned with comparing other well-known techniques with that of PSRMT. Emphasis is placed on the ease and convenience of expressing the mutual impedance integrals of coplanar dipoles in closed form.

FORM 1473 (PAGE 1)
NOV 68
01-807-6811

Security Classification

A-31408

KEY WORDS	LINK A		LINK B		LINK C	
	ROLE	WT	ROLE	WT	ROLE	WT
Computer Program						
Dipole Antennas						
Matrix Methods						
Wire Antennas						

Thesis
B8293 Bryant
c.1
145283
An application of the piecewise-sinusoidal reaction matching technique to linear dipole antennas.